Chemical and Pharmaceutical Bulletin Advance Publication by J-STAGE
DOI:10.1248/cpb.c18-00636

Advance Publication
October 5, 2018

Chem. Pharm. Bull.

Regular Article

Design, Synthesis, and Screening of 5-Aryl-3-(2-(pyrrolyl) thiophenyl)-1, 2, 4-oxadiazoles As Potential Antitumor Molecules on Breast Cancer MCF-7 Cell Line.

Mohammed K. Abd el hameid

Organic Pharmaceutical Chemistry Department, Faculty of Pharmacy, Cairo University, Egypt,

Dedicated to the memory of Dr. Ibrahim Abouleish

© 2018 The Pharmaceutical Society of Japan

Abstract:
The work reported the design and cytotoxic screening of synthetic small molecules: carbonitriles **3a-c**, carboximidamides **4a-c,** and oxadiazoles **5-19** as antitumor molecules. Molecules **4c, 9, 12,** and **14** show promising cytotoxicity profiles against two cell lines higher than prodigiosin (PG). The results of topoisomerase enzyme inhibition assay show that carboximidamide **4c** and oxadiazole **14** display potent inhibitory activity in nano-molar concentration higher than PG. In addition, carboximidamide **4c** and oxadiazoles **9**, **12**, and **14** exhibit antiproliferative activities over MCF-7 cells by cell cycle arrest at G_1 phase and apoptosis inducing activity by increasing cell population percentages at pre G_1 and G_2/M phases as shown by DNA-flow cytometry assay and annexin V analysis. Moreover, measurement of p53 and cell death mediators, show that carboximidamide **4c** and oxadiazoles **9**, **12**, and **14** significantly up-regulate p53, Puma and Bax/Bcl-2 ratio levels. Subsequently, pro-apoptotic activities are confirmed by active caspase 3/7 percentages green fluorescence assay.

Keywords:
DNA intercalators, topoisomerase, thiophene, oxadiazole, breast cancer

1-Introduction:

DNA synthesis has been regarded as one of the most effective targets in cancer cell growth inhibition and apoptosis induction [1]. Generally, all cancer cells are characterized by increasing DNA synthesis that has been mainly referred to up-regulation of DNA topoisomerase (topo) enzymes. Mechanistically, DNA interactive molecules exert their mode of action as DNA synthesis inhibitors either as intercalators or topo inhibitors. Structurally, the common structural basis of these molecules are the polycyclic molecular skeleton either orthogonal or planar required for DNA base pair interaction and enzyme binding. Besides that, the molecular skeletons also have to carry side chains that anchor DNA base pairs and enzyme binding sites by non-covalent interactions [2]. Natural products are important utility in drug discovery as the diversity of their structures inspire the design and the discovery of many drugs [3]. Terthiophene (TER), terpyridine and prodigiosin (PG) (Fig. 1) are natural compounds with an orthogonal tri-arylated molecular skeleton and exhibit potent cytotoxic and pro-apoptotic properties toward a variety of cancer cell lines. Their mode of cytotoxicity is mainly DNA synthesis inhibition [4-8]. Obatoclax (*Teva Pharmaceuticals*) (Fig. 1) is an apoptotic inducer agent over different cancer cell lines and is synthetically derived from PG [8].

Interestingly, the oxazole, isoxazole, and oxadiazole are a privileged core rings in numerous antitumor molecules like MX 74420(*Maxim Pharmaceuticals*), SEW 2871(*EPI Corporation*), VA-62784, and molecule **I** (Fig. 1) [9-13]. These rings represent promising scaffolds in the design of orthogonal DNA interacting agents due to the following reasons. They have a similar configurational ability to act as a rigid spacer or core between two pharmacophoric arms. In addition, these rings are hydrogen bond acceptor (H-bond -A) forming moieties that facilitate binding of molecules with DNA and enzyme binding sites [14]. The mentioned cytotoxic molecules show a common configurational resemblance in their molecular structures as curved or orthogonal poly-aryl ring system composed of core part equipped with two symmetrical or unsymmetrical aryl groups as side chains. P53 upregulated modulator of apoptosis (Puma) is a downstream protein of p53 and is expressed as a secondary effect to DNA damage to induce apoptosis in cancer cells. Puma plays a vital role in the determination of the levels of Bax and Bcl-2 proteins in the cancer cells [15, 16]. Cancer cells resistance to apoptosis induction for the first-line chemotherapy drugs is appeared mainly due to dysfunction in tumor suppressor gene (p53) and up-regulated expression of cell death modulators as the Bcl-2 protein family. Therefore, the discovery of

novel antitumor molecules enhanced apoptosis-inducing activities represents a significant challenge in the oncology research.

[Please insert Fig. 1 about here]

Based on these aforementioned structural similarities and a bio-isosteric relation between benzene, thiophene and azole rings, synthetic small molecules (SSMs) are designed as antitumor agents (Fig. 2). The basic structural skeleton of the lead template is formed from orthogonal 2-(pyrrol-1-yl) thiophene-3-carbonitriles **3a-c** as lead compounds. In addition, thiophene fragments are decorated at C-4 and C-5 positions with three different lipophilic and conformational moieties as dimethyl and tetra-methylene and 4-methoxyphenyl groups to give variable skeletal extensions. Furthermore, the thiophene-3-carbonitriles **3a-c** are grafted with carboximidamide group as H-bond acceptor-donor (A-D) pair forming group via chemical modification of carbonitrile group to reinforce the interaction with the DNA and/or the enzyme binding sites. Besides that, carboximidamide group also is capable of forming a pseudo intramolecular H-bond ring that extended the structural skeleton (model A, carboximidamides **4a-c**). As a final structural modification, the amidoxime group in the conformers **4a-c** is rigidified into oxadiazole ring with the addition of aryl side chains at the C-5 of the core (model B, oxadiazoles **5-19**). The final molecules **5-19** are formed from diaryl oxadiazole skeleton with oxadiazole as core ring with unsymmetrical C-3 and C-5 diaryl groups, C-3 moieties are equipped with 2-(pyrrol-1-yl) thiophen-3yl fragments as bulky side chains and C-5 moieties are substituted phenyl groups (Fig. 2).

[Please insert Fig. 2 about here]

2- Discussion:

2.1. Synthesis:

The steps for synthesis of key starting molecules, intermediates, and the final compounds **3a-c, 4a-c** and **5-19** are illustrated in Charts **1-3.** The rationale of using microwave-assisted organic synthesis (MAOS) in the synthesis of organic molecules is to create a green road towards sustainable development of the chemical industry [17]**.** Since Gewald reported his synthetic protocol for the preparation of 2-aminothiophenes from ketones, active methylene derivatives and sulphur, several reports are published to improve the reaction conditions [18-21]. In the current work, 2-aminothiophenes **2a-c** are prepared in three component reaction via reacting ketones **1a-c** with propane dinitrile and sulfur with using morpholine as a catalyst in n-butanol, (high boiling solvent), instead of ethanol under MAOS conditions (**Chart 1)**.

{Please insert Chart 1 about here]

The structure of thiophene derivatives **2a-c** is confirmed by their reported physical and spectral data [18-20]. Synthesis of pyrrole ring from primary amines using dimethoxytetrahydrofuran (DMTHF) under acid catalyst is known as Clauson-Kaas reaction [22]. In the current work, 2-(pyrrol-1-yl) thiophenes **3a-c** are prepared by reacting 2-aminothiophenes **2a-c** with DMTHF in acetic acid as a dual solvent and catalyst under MAOS conditions (**Chart 1**). Thiophene derivative **3a** is reported as a patent molecule [23], while 2-(pyrrolyl) thiophene **3b** is known in the literature by synthesis under conventional heating with incomplete structural characterization [24]. The preparation of 1, 2, 4-oxadiazole ring is reported from the reaction of carbonitrile, hydroxylamine and acylating agents as carboxylic acids and acid derivatives. The reaction sequence involves the following mechanistic steps, the hydroxylamine is added to aryl nitriles to form amidoximes under base catalyzed conditions. Secondary to that, the amidoximes are coupled with the acylating agents to form oxadiazole ring [25-27].

[Please insert Fig.3 about here]

In this work, oxadiazoles **5-19 (Fig. 3)** are prepared as the following, thiophene-3-carbonitriles **3a-c** are reacted with hydroxylamine hydrochloride using cesium carbonate as a catalyst instead of potassium carbonate, (unstable in M.W irradiation), in n-butanol under MAOS conditions to produce thiophene-3-carboximidamides **4a-c** (**Chart 2).**

[Please insert Chart 2 about here]

The IR spectra of carboximidamides **4a-c**, they show absence of absorption band at 2218 cm^{-1} characteristic to nitrile group cm^{-1} and appearance of absorption bands at the range 3413-3041 cm^{-1} corresponding to NH_2 and OH groups, while ^{1}H-NMR confirm the presence of signals of NH_2 and OH at 4.90-4.95 and 10-63-10.77 ppm. In the second step, amidoximes **4a-c** are acylated with appropriate acid chlorides in ethylene glycol (high boiling solvent) under MAOS conditions to give 3,5-diaryl 1, 2, 4-oxadiazoles **5-19** (**Chart 3**). Several synthetic trails are performed to conduct the preparation of oxadiazoles **10-14** from the nitrile **3b**, hydroxylamine, cesium carbonate and acid chlorides in three-component reaction conditions but the results of all synthetic trails produce the amide of corresponding nitrile **3b**.

[Please insert Chart 3 about here]

2.2-*In vitro* Antiproliferative assay

2.2.1-*In vitro* cell growth inhibition:

The molecules **3a-c**, **4a-c,** and **5-19** are evaluated for antiproliferative activity against breast cancer MCF-7 cells by MTT assay [28] and PG is used as a control compound [7,8]. The obtained results are shown in (**Table 1** and **Fig. 4**).

[Please insert Table. 1 about here]

Carboximidamides **4b**, **4c** and oxadiazoles **9**, **11**, **12**, and **14** with IC_{50} less than (5 μM) against MCF-7 cells are selected for further cytotoxic evaluation on human colon cancer HCT-116 cell lines. The obtained data concerning MCF-7 cells show that molecules **4c, 9, 12,** and **14** exhibit cytotoxic activity in sub-micromolar concentration (IC_{50}: 0.19-0.83 μ M). Inspection of the results according to structural variations between the molecules show the following remarks. Structural modification of thiophene -3-carbo nitrile **3a-c** into thiophene-3-carboximidamides **4a-c** lead to improvement in cytotoxicity results, that may be explained by increasing probability of hydrogen bond formation**.** Regarding groups present at C-4 and C-5 of thiophene ring, carbonitrile **3c** and carboximidamide **4c** exhibit higher activity within molecules **3a-c** and **4a-c,** indicating that common C-4 **(**4-methoxyphenyl) has more contribution in the cytotoxicity than the other two groups. Meanwhile, in model B, 3-(tetrahydrobenzothiophenyl) oxadiazoles **11, 12,** and **14** display higher cytotoxicity among oxadiazoles **5-19,** suggesting that tetra-methylene group at thiophene ring has higher participation in cytotoxicity compared with other C-4 and C-5 substituents at thiophene ring. At the same time, restriction of rotation in amidoxime moiety in thiophene-3-carboximidamides **4a-c** with the addition of different aryl extension may lead to an increase in cytotoxicity as oxadiazoles **10-14** or decrease in cytotoxic activity as in molecules **15-19.** This result may be structurally rationalized as the following, the molecular skeleton of the 2-(pyrrolyl) thiophenes **4a-c** and 3,5-diaryl oxadiazoles **5-19** tolerates only one 4-methoxyphenyl group for good cytotoxic activity. This observation is confirmed by the low cytotoxicity results exhibited by molecules **15-19**, where their precursor **4c** is a potent cytotoxic agent. In respect to the C-5 aryl groups of oxadiazoles **5-19**, molecules **9, 11, 12** and **14** are the most cytotoxic compounds, indicating that 4-methoxyphenyl, 4-chlorophenyl, and 4-bromophenyl have a positive effect on cytotoxicity. In respect to sensitivity of MCF-7 and HCT-116 cells toward the tested molecules, MCF-7 cells are more sensitive than HCT-116 cells to the tested compounds, except **4c** (as indicated by the IC_{50} values). Moreover, thiophene-3-carboximidamide **4c** is more potent than oxadiazole **14** and PG by 2.1- and 4.96- fold over HCT-116 cells. Besides that, oxadiazoles **12** and **14** with C-5 4-bromophenyl and 4-methoxyphenyl groups exhibit good

cytotoxic effect over HCT-116 cells. According to these observations, it is concluded that an orthogonal tri- and tetra-orthogonal aryl molecules **4c** and **14** have antitumor activity over both cell lines.

[Please insert Fig. 4 about here]

2.2.2. *In vitro* topisomerase assay:

Further topo 2β enzymatic inhibition at 5 different doses is performed for the selected molecules: carboximidamide **4b**, **4c,** oxadiazoles **9, 11, 12,** and **14** to evaluate their topo 2β IC_{50} values using PG as a reference. The obtained data show that molecules **4c**, **9**, **12**, and **14** are higher enzyme inhibitors than control that correlate the cytotoxic activity of the compounds to topo enzyme inhibition. In respect to structural activity correlation, 4-(4-methoxyphenyl) thiophene **4c** displays higher topo inhibition than tetrahydrobenzothiophene derivative **4b** indicating that, 4-methoxyphenyl is more active than tetramethylene group at thiophene ring in enzyme inhibition in respect to model A**.** In addition, oxadiazole **14** is more enzyme inhibitor than carboximidamide **4b** by 4.6- fold, suggesting that, the rigid model B display higher activity than rotatable model A. Furthermore, 3-(tetrahydrobenzothiophenyl) oxadiazole **14** shows higher topo enzyme inhibition than 3-(4,5-dimethylthiophenyl) oxadiazole **9**, indicating that tetra-methylene group shows higher activity than dimethyl moieties at thiophene ring in model B. Although 4-(4-methoxphenyl) thiophene -3-carboximidamide **4c** and 5-(4-methoxy phenyl) oxadiazole **9** are from different models they are nearly equipotent in topo inhibition, that confirm the role of 4-methoxyphenyl group in the enzyme inhibition activity. Oxadiazole **14** with C-5(4-methoxyphenyl) group is more potent than other oxadiazoles **11** and **12** with C-5 (chlorophenyl and bromophenyl), confirming the previous finding. Finally, 5-(4-bromophenyl) oxadiazole **12** exhibits higher enzyme inhibition than 5-(4-chlorophenyl) oxadiazole **11,** indicating that the halide nature contributes to enzyme inhibition activity.

[Please insert Fig. 5 about here]

2.2.3. *In vitro* DNA immunofluorescence assay:

On structural basis for SAR studies, carboximidamide **4b**, **4**c and oxadiazoles **9**, and **14** are selected for DNA binding affinity compared with PG, indirect binding pico -green immunofluorescence assay is performed (Fig. 6). In this assay, the fluorescent pico-green dye reversibly binds DNA to form a persistent fluorescent colored complex. When the DNA intercalators are added, the dye is displaced from DNA leading to a decrease in fluorescence [29]. The results show that model A (molecules **4b** and **4c**) have good binding affinity than

model B (**9** and **14**). Unfortunately, the obtained results of histochemical immunoassay are not in agreement with the data of MCF-7 cells IC_{50} and topo enzyme inhibition, so it will be excluded from the predication of final structural activity relationship.

[Please insert Fig. 6 about here]

2.2.4. *In vitro* DNA- flow cytometry and Annexin staining analysis:

To explore the effect of molecules **4b**, **4c**, **9,** and **14** on cell growth inhibition and pro-apoptotic characters, the molecules are subjected to DNA flow cytometry cell cycle analysis. The results are shown in (**Fig. 7).** The distribution pattern of cell cycle phases for MCF-7 cells is a significantly changed after incubation with tested molecules at their IC_{50} compared with PG and untreated cells [30]**.** The molecules induce accumulation percentage of the cells in G_0 phase by 8-, 13-, 9.5- and 15 - fold and G_2/M phases by 1.4-, 1.8-, 1.5-, and 1.8- fold respectively, in comparison with untreated MCF-7 cells, indicating that the tested molecules have cell cycle arrest at G_1 phase and pro-apoptotic activities. In addition, only, molecules **4c**, **14,** and PG induce a significant decrease in the cell population at S phase by 2 -, 1.6- and 1.3-fold respectively, compared with untreated cells. It could be concluding that, tested molecules **4c** and **14** exhibits potent antiproliferative activity than compounds **4b** and **9**.

[Please insert Fig. 7 about here]

The annexin assay further confirms the occurrence of apoptosis induction in MCF-7 cells by the tested molecules. The results are shown in (**Fig. 8**). Results of the assay exhibit that both stages of apoptotic MCF-7 cells (early and late) increase by molecules **4b**, **4c**, **9,** and **14** by 8 -, 11-, 9 -, and 15 - fold compared with untreated cells. Moreover, compound **14** exhibits a profile of strong apoptotic inducer over MCF-7 cells by 1.2- fold than PG. In conclusion, data indicate that molecules **4b**, **4c**, **9,** and **14** are the potent inducer of apoptosis over MCF-7 cells and **14** can induce apoptosis percentage higher than PG, molecule **4c** is slightly less potent than PG, meanwhile compounds **4b** and **9** show equal apoptotic inducing activity to each other and lower than PG.

[Please insert Fig. 8 about here]

2.2.5. *In vitro* ElISA immunoassay for p53 and cell death modulators:

P53 is the main regulator of the intrinsic apoptotic pathway induced by different stimulations via expression of Puma. Therefore, ELISA-immunoassay for p53, Puma, Bax and Bcl-2 measurement in MCF-7 cells for the effect of molecules **4b**, **4c**, **9,** and **14** at their IC_{50} compared with untreated cells and PG is performed. The results are shown in (**Fig. 9 A-E)**. The data indicate that compounds **4b**, **4c**, **9,** and **14** up-regulated p53 levels by 12-, 17-,

19.5-, and 25.7- fold, respectively, higher than untreated cells (**Fig. 9A).** Molecules **4c** and **9** are nearly equivalent in their up-regulation and both are less than **14** and PG**.** Molecule **14** increase p53 level by 1.1- fold higher than PG. Similarly, compounds **4b**, **4c**, **9,** and **14** increase Puma level by 4.5-, 6.5-, 5-, and 7.0-, fold, respectively more than untreated cells (**Fig. 9B)**. Meanwhile, compound **14** increase level of Puma higher than PG by 1.2-fold and **4c** is equipotent compound to PG. This increasing in p53 and Puma levels most probably caused by DNA damage effect of the tested compounds.

Subsequently, Compounds **4b, 4c**, **9,** and **14** increase Bax/Bcl-2 ratio by 4.3-, 8.5-, 3.5, and 9.5- fold to untreated cells. Molecule **14** has higher Bax/Bcl-2 ratio by 1.3-fold than PG (**Fig. 9C, D, and E)**. The data obtained from p53, Puma and Bax/Bcl-2 ratio support the previous elucidated structure-activity correlation between the tested compounds.

[Please insert Fig. 9 about here]

2.2.6. *In vitro* green flow cytometry assay for active caspase 3/7 percentage:

Caspase-3/7 enzymes are the terminal downstream of caspases activation that catalyzed the apoptosis process either intrinsic or extrinsic pathways. Treated MCF-7 cells with compounds **4b, 4c, 9, 14,** and PG at their IC_{50} are subjected to green immunofluorescence to measure active caspase-3/7 percentages. The data show that carboximidamides **4b**, **4c** and oxadiazoles **9, 14** increase active caspase-3/7 percentages by 3-, 8.6-, 6.4-, 10-fold, respectively, more than untreated MCF-7 cells as seen in (**Figs. 10)**. Additionally, carboximidamide **4c** increase caspase 3/7 higher than oxadiazole **9.** Moreover, carboximidamide **4c** and oxadiazole **14** increase caspase-3/7 percentages by 1.1- and 1.3- fold than PG. As a final conclusion from biological screening results, molecules **4b**, **4c**, **9,** and **14** are cytotoxic agents and trigger apoptosis induction in MCF-7 cells as a secondary effect to DNA damage with subsequent secondary increasing in p53 and Puma levels that overcome the resistance conferred by Bcl-2 proteins via an increase in Bax/Bcl-2 ratio and activation of terminal caspase 3/7 proteins.

[Please insert Fig. 10 about here]

3-Conclusion:

Briefly, a small library of carbonitriles **3a-c**, carboximidamides **4a-c** and oxadiazoles **5-19** is designed as potential anticancer molecules. The following steps demonstrate the synthetic protocol, where thiophene derivatives **2a-c** are synthesized in three component Gewald reaction. In addition, the amino group of thiophene-3-carbonitrile **2a-c** is cyclized

into pyrrole ring (thiophenes **3a-c)** using DMTHF. Furthermore, thiophene-3-nitriles **3a-c** are converted to thiophene-3-carboxmidoximes **4a-c** via reaction with hydroxyl amine. Finally, carboximidamides **4a-c** are cyclized into oxadiazoles **5-19** by reaction with different aryl acid chlorides. The cytotoxicity results regarding MCF-7 cells show that, carboximidamide **4c** and oxadiazoles **9**, **12** and **14** show IC_{50} in sub-micmolar concentration and more potent by 2.3-, 4-, 2.5-, and 10 -fold than PG. Meanwhile, molecules **4c**, **12,** and **14** exhibit higher cytotoxic activity by 5 -, 1.8-, and 2.4- fold, respectively than control on HCT-116 cells. The antiproliferative activity of tested molecules is correlated to topoisomerase enzyme inhibition, where carboximidamide **4c** and oxadiazoles **9** and **14** are potent enzyme inhibitors by 2-, 2 -, and 2.7 -fold, respectively than PG. Moreover, the cell cycle flow cytometry analysis displays that compounds **4c, 9, 11,** and **14** induce cell cycle arrest at G_1 phase of MCF-7 cells. In addition, molecule **14** is stronger apoptotic inducers than PG, as demonstrated by the results of Annexin assay. ELISA measurement for p53 and cell death modulators (Puma, Bax and Bcl-2) show that carboximidamide **4c** and oxadiazoles **9, 12,** and **14** induce upregulation of p53 and increase Puma, and Bax/Bcl-2 ratio levels. The results of the green fluorescence assay exhibit that carboximidamide **4c** and oxadiazoles **9**, **11,** and **14** trigger apoptosis induction via increase active caspase 3/7 percentage. Finally, compounds carboximidamide **4c** and oxadiazole **14** represent promising antitumor and apoptosis-inducing agents.

4- Experimental:

4.1. Synthesis:

4. 1. 1. Apparatus:

Melting points of the synthesized molecules are measured with a Stuart melting point apparatus and are uncorrected. The NMR spectra of molecules are measured by Varian Gemini-300BB 300 MHz FT-NMR spectrometers (Varian Inc., Palo Alto, CA). ^{1}H and ^{13}C spectra are run at 400 and 100 MHz, respectively, in deuterated dimethyl sulphoxide (DMSO-d_6). IR spectra of molecules are recorded with a Bruker FT-IR spectrophotometer. Electron impact (EI) mass spectra of molecules are measured on Hewlett Packard 5988 spectrometer. The analysis of elements is carried out at The Regional Center for Mycology and Biotechnology, Al-Azhar University, Egypt. Reactions progress is monitored by thin layer chromatography (TLC) on silica gel precoated plates. The solvent system used for TLC is hexane–ethyl acetate (8.5: 1.5 ml) mixture and the appeared spots are visualized by UV lamp. Silica gel (200–300) mesh is used for Column chromatography. Unless otherwise noted,

all solvents and reagents are commercially available and used without further purification. The M.W. work synthesis workstation is Sieno-Mass-II microwave (M.W.) with the specification (2.45GMHz, 1000 W).

4.1.2. Synthesis of 2-amino-thiophene-3-carbonitriles 2a-c:

Starting materials **2a-c** are prepared via Gewald three-component reaction using n-butanol as high boiling solvent instead of ethanol, in brief, a mixture of appropriate ketones **1a-c** (20.0 mmol), propane dinitrile (3.39 g, 30.0 mmol), and sulfur (3.2 g 10.0mmol) in *n*-butanol (15 ml) is stirred and morpholine (2.61 g, 30.0 mmol) is added dropwise at room temperature with cooling in ice bath. After that, the mixture is heated at 150 ^{0}C for 10 min in a M.W. reactor. The reaction mixture is subjected to cooling to room temperature. After cooling, petroleum ether (20 ml) is added to the mixture and the formed brown precipitate is crystallized from ethanol and afford thiophenes **2a-c.** The structure of 2-aminothiophenes **2a-c** is confirmed by their reported physical and spectral data **2a** [19], **2b** [18] and **2c** [20].

4.1.3. Synthesis of 2-(1H-pyrrol-1-yl) thiophene-3-carbonitriles 3a-c:

A mixture of dimethoxytetrahydrofuran (DMTHF) (0.82 g, 6.2 mmol) and glacial acetic (3 ml) is stirred for 5 min at room temperature, followed by the addition of thiophene-3-carbonitriles **2a-c** (0.62 mmol). The reaction mixture is heated at 100 ^{0}C for 15 min in the M.W. reactor. After cooling, the reaction mixture is diluted with H_2O (20 ml) and the solid formed is crystallized from ethanol to give thiophenes **3a-c.**

4.1.3.1. 4, 5-Dimethyl-2-(1H-pyrrol-1-yl) thiophene-3-carbonitrile (3a)*:* Yield: 0.9 g (74 %) white crystal; m.p. 50-53^{o}C. ^{1}H-NMR (DMSO-d_6), δ:2.24 (s, 3H, CH_3), 2.27 (s, 3H, CH_3), 6.27-6.49 (t, 2H, ArH), 6.52-6.59 (d, 2H, 8.7 Hz, ArH) ppm. ^{13}C-NMR (DMSO-d_6), δ: 9.9, 12.1, 84.6, 108.4, 115.4, 116.0, 123.2, 135.0, 158.7. IR (KBr, ν cm^{-1}): 2984-2896 (aliph.CH) , 2215 (CN). Anal.Calcd.for $C_{11}H_{10}N_2S$ (202.28): C, 65.32; H, 4.98; N, 13.85; Found: C, 65.29; H, 4.84 ; N, 13.72.

4.1.3.2. 2-(1H-Pyrrol-1-yl)-4, 5, 6, 7-tetrahydrbenzo[b]thiopthene-3-carbonitrile (3b): Yield: 1.1g (81 %) white crystal ; m.p. 73-76^{o}C (lit ,63-65^{o}C)[24]. ^{1}H-NMR (300 MHz, DMSO-d_6), δ: 1.73-1.79 (m, 4H, $2CH_2$), 2.65-2.69 (m, 4H, $2CH_2$), 6.18-6.19 (m, 2H, ArH), 6.91-6.92 (m, 2H, ArH) ppm. ^{13}C-NMR (DMSO-d_6), δ: 20.4, 22.9, 23.4, 24.5, 84.0, 108.5, 115.3, 123.2, 134.5, 141.0, 158.1.

4.1.3.3. 3-(4-Methoxyphenyl)-2-(1H-pyrrol-1-yl) thiophene-3-carbonitrile (3c) : Yield: 1.2 g(76 %), white crystal; m.p. 122-123^{o}C. ^{1}H-NMR (DMSO-d_6), δ: 3.71(s, 3H, CH_3), 6.40-6.50(m, 3H, ArH), 6.91-7.05 (m, 4H, ArH), 7.32-7.45 (m, 2H, ArH) ppm. ^{13}C-NMR (DMSO-

d_6), δ: 56.40, 82.3, 108.5, 115.9, 117.9, 123.7, 124.3, 127.8, 128.0, 129.4, 141.2, 160.2. IR (KBr, ν cm^{-1}): 3023 (arom.CH), 2983-2892 (aliph.CH), 2218(CN); Anal.Calcd.for $C_{16}H_{12}N_2OS$ (280.34): C, 68.55; H, 4.31; N, 9.99; Found: C, 68.29; H, 4.64 ; N, 10.12.

4.1.4. *N*-Hydroxy-2-(1H-pyrrol-1-yl) thiopthene-3-carboximidamides 4a-c.

Thiophene 3-carbonitrile derivatives **3a-c** (8 mmol) are dissolved in *n*-butanol (15 ml) and treated with $Cs\,CO_3$ (5.2 g, 16 mmol) and hydroxyl amine hydrochloride (1.0 g, 14.8 mmol), then the reaction mixture is stirred for 5 min at room temperature. The reaction mixture is heated at 140 ^{0}C for 20 min in M.W. reactor. After cooling, diethyl ether (20 ml) is added to the reaction mixture and the solid formed is subjected to filtration and dried under vacuum to produce carboximidamides **4a-c**.

4.1.4.1. *N*-Hydroxy-4, 5-dimethyl-2-(1H-pyrrol-1-yl) thiopthene-3-carboximidamide (4a): Yield: 1.1 g (59 %) brown solid; m.p. 250-253^{o}C. ^{1}H-NMR (DMSO-d_6), δ: 2.25 (s, 3H, CH_3), 2.31 (s, 3H, CH_3), 4.95 (s, 1H, D_2O exchangeable), 6.23-6.38 (m, 1H, ArH), 6.44-6.49 (d, 1H, 8.7 Hz, ArH), 6.95-6.97 (d, 2H,ArH), 10.63 (s,1H, D_2O exchangeable), 10.73 (s,1H, D_2O exchangeable) ppm. ^{13}C-NMR (DMSO-d_6), δ: 10.4, 10.9, 108.3, 120.7, 123.0, 131.5, 134.0, 136.0, 163.2. IR (KBr, ν cm^{-1}): 3412-3090 (NH & OH), 3054 (arom.CH), 2983-2891 (aliph.CH). Anal.Calcd.for $C_{11}H_{13}N_3OS$ (235.31): C, 56.15; H, 5.57; N, 17.86; Found: C, 56.28; H, 5.71 ; N, 17.61.

4.1.4.2. *N*-Hydroxy-2-(1H-pyrrol-1-yl)-4, 5, 6, 7-tetrahydrobenzo[b]thiopthene-3-carboximidamide (4b): Yield: 1.40g (67 %), yellow solid; m.p. 262-265^{o}C. ^{1}H-NMR (DMSO-d_6), δ: 1.60-1.78 (m, 4H, $2CH_2$), 2.72-2.79, (m, 4H, $2CH_2$), 4.90 (s, 2H, D_2O exchangeable), 6.14-6.27 (m, 2H, ArH), 6.91-6.97(m, 2H, ArH), 10.77 (s, 1H, D_2O exchangeable) ppm. ;^{13}C-NMR (DMSO-d_6), δ: 20.4, 23.4, 24.5, 24.6, 108.3, 119.6, 123.1, 127.7, 135.6, 137.4, 163.2. IR (KBr, ν cm^{-1}): 3413-3110 (NH &OH), 3054 (arom.CH), 2984-2890 (aliph.CH). Anal.Calcd.for $C_{13}H_{15}N_3OS$ (261.09): C, 59.74; H, 5.79; N, 16.08; Found: C, 59.82.; H, .93 ; N, 16.11.

4.1.4.3. *N*-Hydroxy-4-(4-methoxyphenyl)-2-(1H-pyrrol-1-yl) thiopthene-3-carboximidamide (4c): Yield: 1.45g (58 %), yellow solid; m.p. 286-289^{o}C. ^{1}H-NMR (300 MHz, DMSO), δ : 3.86 (s, 3H, CH_3), 4.92 (s, 2H, D_2O exchangeable), 6.19-6.24 (m, 2H, ArH), 6.34-6.46 (m, 1H, ArH), 6.80-6.85 (s, 2H, ArH), 6.91-7.07 (s, 2H, ArH), 7.39-7.47 (m, 2H, ArH), 10.76 (s, 1H, D_2O exchangeable) ppm. ^{13}C-NMR (DMSO-d_6), δ : 56.4, 108.2, 114.8, 118.3, 123.1, 123.3, 127.0, 128.5, 137.4, 138.2, 160.6, 163.4. IR (KBr, ν cm^{-1}): 3373-

3041 (-NH &OH), 3054 (arom.CH), 2997-2983 (aliph.CH). Anal.Calcd.for $C_{16}H_{15}N_3O_2S$ (313.37): C, 61.32; H, 4.82; N, 13.41; Found: C, 61.86; H, 4.94 ; N, 13.33.

4.1.5. Synthesis of 5-aryl-3-(2-(1H-pyrrol-1-yl)-thiophen-3-yl)-1, 2, 4-oxadiazoles 5-19.

Thiophene-3-carboximidoximes **4a-c** (0.8 mmol) are dissolved in ethylene glycol (10 ml), then the appropriate acid chloride (0.8 mmol) is added with continuous cooling and stirring of the reaction mixture. The reaction mixture is heated at 200 ^{0}C for 5 min. After cooling, saturated aqueous $NaHCO_3$ solution (10 ml) is added to the reaction mixture. Then, the mixture is extracted with ethyl acetate (3 × 15 ml) and the combined organic layers are dried and evaporated under reduced pressure. The obtained solid is subjected by column chromatography using a mixture of ethyl acetate: pet. ether (1:9) to give oxadiazoles **5-19.**

4.1.5.1. 3-[4, 5-Dimethyl-2-(1H-pyrrol-1-yl) thiophen-1-yl]-5-phenyl-1, 2, 4-oxadiazole(5): Yield: 0.19 g (75 %), yellow powder; m.p. 98-100^{o}C.^{1}H-NMR(DMSO-d_6), δ: 2.23 (s, 3H, CH_3), 2.33 (s, 3H, CH_3), 6.31-6.46 (m, 2H, ArH), 6.50-6.61 (m, 3H, ArH), 6.65-7.28 (m, 2H, ArH), 7.29-7.39 (m, 2H, Ar H) ppm.^{13}C-NMR (DMSO-d_6), δ: 11.1, 13.2, 110.4, 117.3, 124.0, 124.2, 127.5, 128.7, 129.2, 131.7, 134.7, 139.4, 143.5, 166.5, 176.9 ppm. IR (KBr, ν cm^{-1}): 3021 (arom.CH) , 2993-2981 (aliph.CH). MS (m/z, %): 321.06 (M^+, 15.21), 315.19 (100). Anal.Calcd.for $C_{18}H_{15}N_3OS$ (321.4): C, 67.27; H, 4.70; N, 13.07; Found: C, 67.28; H, 4.74 ; N, 13.31.

4.1.5.2. 5-(4-Chlorophenyl)-3-[4, 5-dimethyl-2-(1H-pyrrol-1-yl)thiophen-3-yl]-1, 2, 4-oxadiazole (6): Yield: 0.16 g (55%), brown powder. m.p. 153-157^{o}C ;^{1}H-NMR (DMSO-d_6), δ: 2.28 (s, 3H, CH_3), 2.31 (s, 3H, CH_3), 6.54 (s, 2H, ArH), 7.05-7.08 (d, 2H, ArH), 7.38-7.40 (d, 2H, ArH), 7.73 (s, 2H, ArH) ppm. ^{13}C-NMR (DMSO-d_6) δ: 11.1, 13.2, 110.4, 124.0, 124.2, 127.5, 128.7, 129.2, 131.7, 134.7, 139.5, 143.5, 166.4, 176.9 ppm. IR (KBr,νcm^{-1}) : 3021 (arom.CH), 2997-2979 (aliph.CH). MS (m/z, %): 355.22 (M^+, 10.25), 331.32 (100). Anal.Calcd.for $C_{18}H_{14}ClN_3OS$ (355.84): C, 60.76; H, 3.97; N, 11.81; Found: C, 60.70; H, 3.84 ; N, 11.71.

4.1.5.3. 5-(4-Bromophenyl)-3-[4, 5-dimethyl-2-(1H-pyrrol-1-yl) thiophen-3-yl]1, 2, 4-oxadiazole (7): Yield: 0.19 g (59 %), yellowish white powder. m.p. 132-135^{o}C. ^{1}H-NMR (DMSO-d_6) , δ : 2.26 (s, 3H, CH_3), 2.30 (s, 3H, CH_3), 6.55-6.96 (m,4H, ArH), 7.25-7.66 (m, 4H, ArH) ppm. ^{13}C-NMR (DMSO-d_6), δ: 11.1, 13.2, 110.4, 124.0, 125.4, 126.4, 127.5, 129.3, 131.7, 134.8, 139.5, 143.5, 166.5, 176.9 ppm. IR (KBr, νcm^{-1}): 3019 (arom.CH), 2995-2980 (aliph.CH) . MS (m/z, %): 399.12 (M^+, 15.28), 345.51 (100) .Anal.Calcd.for $C_{18}H_{14}BrN_3OS$ (400.29) : C, 54.01; H, 3.53; N, 10.50, found : C, 54.22; H, 3.61; N, 10,38.

4.1.5.4. 3-[4, 5-Dimethyl-2-(1H-pyrrol-1-yl)thiophen-3-yl]-5-(4-tollyl)1, 2, 4-oxadiazole (8): Yield: 0.13 g (49 %), yellow powder ; m.p. 88-90^{o}C . ^{1}H-NMR (DMSO-d_6), δ : 2.30 (s, 3H, CH_3), 2.34 (s, 3H, CH_3), 2.40 (s, 3H, CH_3), 6.55-6.89 (m, 4H, ArH), 7.21-6.26 (m, 2H, ArH), 7.54-7.63 (m, 2H, ArH) ppm.^{13}C-NMR (DMSO-d_6) δ: 11.1, 13.2, 22.1, 110.4, 124.0, 124.1, 127.5, 128.7, 129.2, 131.7, 134.7, 139.4, 143.5, 166.5, 175.8 ppm. IR (KBr, νcm^{-1}): 3027 (arom.CH), 2997-2984 (aliph.CH) . MS (m/z, %): 334.11 (M^+, 35.51), 301.54 (100). Anal.Calcd.for $C_{19}H_{17}N_3OS$ (335.42): C, 68.03; H, 5.11;N, 12.53; Found: C, 68.14; H, 5.23 ; N, 12.63.

4.1.5.5.3-[4,5-Dimethyl-2-(1H-pyrrol-1-yl)thiophen-3-yl]-5-(4-methoxyphenyl)-1, 2, 4-oxadiazole (9): Yield: 0.16 g (56 %) ,yellow powder; m.p. 167-170^{o}C ;^{1}H-NMR (DMSO-d_6), δ: 2.24 (s, 3H, CH_3), 2.38 (s, 3H, CH_3), 3.80 (s, 3H, -OCH_3), 6.33-6.42 (m, 2H, ArH), 6.44-6.60 (m, 1H, ArH), 6.61-6.68 (m, 3H, ArH), 6.82-6.93 (m, 2H, Ar H) ppm, ^{13}C-NMR (DMSO-d_6), δ: 11.1, 13.2, 57.4, 110.4, 124.1, 125.2, 126.4, 127.5, 129.2, 131.7, 134.7, 139.4, 143.4, 166.4, 176.8 ppm. IR (KBr,νcm^{-1}): 3020 (arom.CH), 2996-2982 (aliph.CH). MS (m/z, %): 351.17 (M^+, 60.22), 315.41 (100). Anal.Calcd.for $C_{19}H_{17}N_3O_2S$ (351.42): C, 64.94; H, 4.88;N, 11.96; Found: C, 64.74; H, 4.68 ; N, 11.76.

4.1.5.6.3-[2-(1H-Pyrrol-1-yl)-4, 5, 6, 7-tetrahydrobenzo[b]thiophen-3-yl]-5-phenyl-1, 2, 4-oxadiazole (10)*:* Yield: 0.22 g (79 %), orange powder; m.p. 141-146^{o}C.^{1}H-NMR (DMSO-d_6), δ: 1.73-1.82 (m, 4H, $2CH_2$), 2.71-2.91 (m, 4H, $2CH_2$), 6.86-7.01 (m, 2H, ArH), 7.13-7.29 (m, 3H, ArH), 7.37-7.53 (m, 4H, ArH) ppm; ^{13}C-NMR (DMSO-d_6), δ : 22.3, 22.6, 25.7, 25.9, 115.0, 117.6, 127.0, 128.3, 131.7, 132.3, 133.4, 134.0, 135.7, 145.6, 164.0, 176.6 ppm. IR (KBr, νcm^{-1}) : 3015 (arom.CH), 2993-2980 (aliph.CH). MS (m/z, %): 347.13 (M^+, 10.58), 151.22 (100). Anal.Calcd.for $C_{20}H_{17}N_3OS$ (347.43): C, 69.14; H, 4.93;N, 12.09; Found: C, 69.34; H, 4.90 ; N, 12.11.

4.1.5.7.3-[2-(1H-Pyrrol-1-yl)-4, 5, 6, 7-tetrahydrobenzo[b]thiophen-3-yl]-5-(4-chloro phenyl)-1, 2, 4-oxadiazole (11): Yield: 0.19 g (63 %), yellow powder; m.p. 152-156^{o}C. ^{1}H-NMR (DMSO-d_6), δ: 1.75-1.80 (m, 4H, $2CH_2$), 2.61-2.91 (m, 4H, $2CH_2$), 6.47-6.52 (m, 1H, ArH), 6.67-6.79 (m, 4H, ArH), 7.30-7.43 (m, 3H, ArH) ppm.^{13}C-NMR (DMSO-d_6):δ: 22.5, 22.7, 25.8, 26.0, 111.2, 122.3, 123.1, 124.2, 125.1, 127.3, 128.1, 129.3, 140.3, 142.4, 166.7, 176.8 ppm. IR (KBr, νcm^{-1}): 3034 (arom.CH), 2997-2981 (aliph.CH). MS (m/z, %): 381.16 (M^+, 10.83), 187.32 (100). Anal.Calcd.for $C_{20}H_{16}ClN_3OS$ (381.88): C, 62.90; H, 4.22; N, 11.00; Found: C, 62.80; H, 4.04 ; N, 10.81.

4.1.5.8. 3-[2-(1H-Pyrrol-1-yl)-4, 5, 6, 7-tetrahydrobenzo[b]thiophen-3-yl]-5-(4-bromo phenyl)-1, 2,4-oxadiazole (12): Yield: 0.23 g (66 %), red powder; m.p.121-125^{o}C. ^{1}H-NMR (DMSO-d_6), δ: 1.74-1.80 (m, 4H, $2CH_2$), 2.67-2.73 (m, 4H, $2CH_2$), 6.16-6.20 (m, 1H, ArH), 6.38 (s, 3H, ArH), 6.95-6.98 (m, 2H, ArH), 7.24 (s, 1H, ArH), 7.45 (s, 1H, ArH) ppm; ^{13}C-NMR (DMSO-d_6):δ: 22.6, 22.8, 25.2, 26.0, 106.0, 121.2, 121.8, 129.5, 130.7, 132.0, 133.7, 134.8, 136.1, 140.0 , 166.2, 175.4 ppm. IR (KBr, νcm^{-1}): 3034 (arom.CH), 2994-2983 (aliph.CH). MS (m/z, %): 425.44 (M^+, 5.98), 331.61 (100). Anal.Calcd.for $C_{20}H_{16}BrN_3OS$ (426.33): C, 56.34; H, 3.78;N, 9.86; Found: C,56.44; H, 3.84 ; N, 9.71.

4.1.5.9. 3-3-[2-(1H-Pyrrol-1-yl)-4, 5, 6, 7-tetrahydrobenzo[b]thiophen-3-yl]-5-(4-tolyl)-1, 2, 4-oxadiazole (13): Yield: 0.17 g (60 %), red powder; m.p. 142-146^{o}C. ^{1}H-NMR (DMSO-d_6), δ: 1.76-1.95 (m, 4H, $2CH_2$), 2.15 (s, 3H, CH_3), 2.65-2.91 (m, 4H, $2CH_2$), 6.44-6.60 (m, 2H, ArH), 6.62-6.84 (m, 3H, ArH), 6.99-7.05 (m, 2H, ArH), 7.16-7.46(m, 1H, ArH) ppm.^{13}C-NMR (DMSO-d_6) , δ: 21.4, 22.6 , 22.8, 25.2, 26.0, 112.2, 121.0, 124.6, 125.8, 128.8, 131.4, 133.5, 138.1, 140.9, 141.0, 167.7, 173.1 ppm. IR (KBr, νcm^{-1}): 3031 (arom.CH), 2995-2980 (aliph.CH). MS (m/z, %): 361.21 (M^+, 35.65), 257.51 (100). Anal.Calcd.for $C_{21}H_{19}N_3OS$ (361.46): C, 69.78; H, 5.39; N, 11.63; Found: C, 69.88; H, 5.44 ; N, 11.71.

4.1.5.10. 3-3-[2-(1H-Pyrrol-1-yl)-4, 5, 6, 7-tetrahydrobenzo[b]thiophen-3-yl]-5-(4-methoxyphenyl)-1, 2, 4-oxadiazole (14): Yield: 0.18g (58 %) , buff solid; m.p. 133-137^{o}C; ^{1}H-NMR (DMSO-d_6), δ: 1.74-1.80 (m, 4H, $2CH_2$), 2.60-2.69 (m, 4H, $2CH_2$), 3.84 (s, 3H, -OCH_3), 6.16-6.20 (m, 2H, ArH), 6.21-6.38 (m, 2H, ArH), 6.95-6.98 (m, 2H, ArH), 7.23-7.56 (m, 2H, ArH) ppm. ^{13}C-NMR (DMSO-d_6), δ: 22.2, 22.9, 25.4, 25.6, 56.5, 105.9, 112.2, 121.4, 126.0, 128.7, 132.6, 133.6, 135.6, 145.7, 153.1, 166.0, 176.7 ppm. IR (KBr, νcm^{-1}): 3024 (arom.CH) , 2990-2982 (aliph.CH) . MS (m/z, %): 377.12 (M^+, 10.05), 343.56 (100). Anal.Calcd.for $C_{21}H_{19}N_3O_2S$ (377.46): C, 66.82; H, 5.07;N,11.13; Found: C, 66.77; H, 5.14 ; N, 11.10.

4.1.5.11. 5-Phenyl-3-(4-methoxyphenyl-2-(1H-pyrrol-1-yl)thiophen-3-yl)-1, 2, 4-oxadiazole (15): Yield: 0.23 g (71%), orange powder; m.p. 122-126^{o}C. ^{1}H-NMR (DMSO-d_6), δ: 3.84 (s, 3H, -OCH_3), 6.20-6.34 (m, 2H, ArH), 6.36-6.66 (m, 2H, ArH), 6.70-6.73 (m, 3H, ArH), 6.98-7.08 (m, 3H, ArH), 7.14-7.18 (m, 2H, ArH), 7.53-7.67 (m, 2H, ArH) ppm.^{13}C-NMR (DMSO-d_6):δ: 55.8, 111.7, 112.0, 117.1, 118.7, 119.5, 121.5, 121.6, 122.7, 129.5, 130.7, 132.5, 134.8, 135.9, 136.8, 149.0, 165.9, 176.6 ppm. IR (KBr, νcm^{-1}): 3028 (arom.CH), 2998-2980 (aliph.CH) .MS (m/z, %): 399.10 (M^+, 39.23), 377.16 (100). Anal.Calcd.for $C_{23}H_{17}N_3O_2S$ (399.46): C, 69.15; H, 4.29; N, 10.52; Found: C, 69.23; H, 4.50 ; N,10.71.

4.1.5.12. 5-(4-Chlorophenyl)-3-[4-(4-methoxyphenyl)-2-(1H-pyrrol-1-yl)thiophen-3-yl)-1, 2, 4-oxadiazole (16): Yield: 0.20 g (59%), red powder; m.p. 166-170°C. ^{1}H-NMR (DMSO-d_6), δ: 3.82 (s, 3H, OCH_3), 6.26-6.36 (m, 3H, ArH), 6.76-6.79 (m, 4H, ArH), 6.99-7.29 (m, 4H, ArH), 7.32-7.39(m, 2H, ArH) ppm. ^{13}C-NMR (DMSO-d_6): ^{13}C NMR (DMSO-d_6), δ: 56.5, 106.0, 112.3, 113.2, 121.2, 129.5, 130.6, 132.0, 132.1, 134.9, 136.8, 140.0, 146.0, 149.0, 153.3, 167.0, 175.4 ppm. IR (KBr, νcm^{-1}): 3031 (arom.CH) , 2993-2982 (aliph.CH) . MS (m/z, %): 433.10 (M^+, 5.25), 367.33 (100). Anal.Calcd.for $C_{23}H_{16}ClN_3O_2S$ (433.91): C, 63.66; H, 3.72; N, 9.68; Found: C, 63.88; H, 3.84 ; N, 9.71.

4.1.5.13. 5-(4-Bromophenyl)-3-[4-(4-methoxyphenyl)-2-(1H-pyrrol-1-yl)thiophen-3-yl)-1, 2, 4-oxadiazole (17): Yield: 0.25 g (65%) ,brown solid; m.p. 172-173°C. ^{1}H-NMR (DMSO-d_6), δ: 3.81 (s, 3H, -OCH_3), 6.20-6.21 (m, 2H, ArH), 6.53-6.56 (m, 2H, ArH), 6.88-7.09 (m, 5H, ArH), 7.21-7.23 (m, 2H, ArH), 7.40-7.42 (m, 2H, ArH)ppm. ^{13}C-NMR (DMSO-d_6), δ: 56.2, 105.4, 106.2, 107.2, 112.3, 113.0, 118.3, 122.0, 127.9, 128.0, 129.4, 132.2, 135.0, 139.8, 146.0, 165.4, 176.8 ppm. IR (KBr, νcm^{-1}): 3028 (arom.CH) , 2992-2980 (aliph.CH). MS (m/z, %): 477.12 (M^+, 35.21), 413.23 (100). Anal.Calcd.for $C_{23}H_{16}BrN_3O_2S$ (478.36): C, 57.75; H, 3.37; N, 8.78; Found: C, 57.65; H, 3.30 ; N, 8.70.

4.1.5.14. 5-(4-Methylphenyl)-3-[4-(4-methoxyphenyl)-2-(1H-pyrrol-1-yl)thiophen-3-yl]-1, 2, 4-oxadiazole (18): Yield: 0.19 g (58 %), yellowish white powder; m.p. 152-156°C. ^{1}H-NMR (DMSO-d_6):δ: 2.38 (s, 3H, CH_3), 3.78 (s, 3H, -OCH_3), 6.33-6.36 (m, 3H, ArH), 6.68-6.94 (m, 2H, ArH), 7.05-7.18(m, 3H, ArH), 7.20-7.44 (m, 3H, ArH), 7.55(s, 1H, ArH, 7.58 (s, 1H, ArH). ^{13}C-NMR (DMSO-d_6), δ: 20.6, 56.6, 106.0, 117.7, 120.0, 124.6, 127.0, 128.6, 133.6, 135.7, 139.1, 141.1, 142.5, 145.6, 153.2, 153.7, 167.7, 174.7 ppm.IR (KBr, νcm^{-1}) : 3012 (arom.CH), 2996-2987 (aliph.CH). MS (m/z, %): 413.11 (M^+, 25.22), 347.16 (100). Anal.Calcd.for $C_{24}H_{19}N_3O_2S$ (413.49): C, 69.71; H, 4.63; N, 10.16; Found: C, 69.88; H, 4.44 ; N, 10.17.

4.1.5.15. 5-(4-Methoxyphenyl)-3-(4-methoxyphenyl-2-(1H-pyrrol-1-yl)thiophen-3-yl)-1, 2, 4-oxadiazole (19): Yield: 0.16 g (46%), red powder; m.p. 190-193°C. ^{1}H-NMR (DMSO-d_6), δ : 3.67 (s, 3H, -OCH_3), 3.78 (s, 3H, -OCH_3), 6.26-6.38 (m, 4H, ArH), 6.41-6.53 (m, 3H, ArH), 6.56-6.95 (m, 3H, ArH), 7.07-7.55 (m, 3H, ArH). IR (KBr, νcm^{-1}) : 3022 (arom.CH) , 2991-2976 (aliph.CH). MS (m/z, %): 429.46 (M^+, 10.21), 347(100). Anal.Calcd.for $C_{24}H_{19}N_3O_3S$ (429.49): C, 67.12; H, 4.46; N, 9.78; Found: C, 67.34; H, 4.74 ; N, 9.71.

4.2- *In vitro* Antiproliferative assay:

4.2.1. *In vitro* cell growth inhibition:

4.2.1.1. Materials:

MCF-7 and HCT-116 cell lines are obtained from american type culture collection. Tumor cells are cultured using DMEM (Invitrogen/Life Technologies) supplemented with10 ug/ml of insulin (Sigma), 10% FBS (Hyclone), and 1% penicillin-streptomycin. Prodigiosin as positive control and all other chemicals and reagents are purchased from Sigma or Invitrogen.

4.2.1.2. Methodology of cell growth inhibition assay:

For antitumor activity, the MCF-7 cells are incubated in the medium in Corning® 96-well tissue culture plates for 24 hr. The tested molecules **3a-c**, **4a-c, 5-19** and PG are then added into 96-well plates at different concentrations for each molecule. Different vehicle controls with media are run for each 96 well plates as a control. After incubating for 24 h, the numbers of viable cells are determined by the tetrazolium MTT (3-(4, 5-dimethylthiazolyl-2)-2, 5-diphenyltetrazolium bromide) assay [28]. The optical density is recorded at 590 nm with the microplate reader (Sun Rise, TECAN, Inc, USA) to determine the number of viable cells. The relation between the percentages of surviving cells and drug concentration is plotted to get the survival curve of MCF-7 cells after treatment with the specified compound, IC_{50} is estimated from graphic plots of the dose -response curve for each concentration using Graph Pad Prism software. The assay is repeated three times.

4.2.2. *In vitro* topoisomerase 2β enzymes assay:

4.2.2.1. Materials:

The following materials served as the enzyme sources, Poly (Glu, Tyr) sodium salt (4:1, Glu: Tyr) (Sigma#P7244) served as the standardized substrate & Kinase-Glo Plus Luminescence kinase assay kit (Promega # V3772) is used. The assay is performed using Kinase-Glo Plus luminescence kinase assay kit (Promega).

4.2.2.2.* Methodology *:

The tested molecules **4b**, **4c**, **9**, **11**, **12**, **14** and PG are diluted to 100 µl in DMSO (10%) and 5 µl of the solution is added to a 50 µl enzyme reaction until e final concentration of DMSO is 1% in all of the reactions. The enzymatic reactions are conducted at 30^{o}C for 40 minutes. The reaction mixture contains enzyme substrate and respective kinases. After the enzymatic reaction, 50 µl of enzyme-Glo Plus luminescence topoisomerase assay solution (Promega) is added to each reaction and the plate is incubated for 5 minutes at room temperature. Luminescence signal is measured using a BioTek Synergy 2 microplate reader.The

luminescence data are analyzed using the computer software, Graphpad Prism. The difference between luminescence intensities in the absence of topoisomerase (Lu_t) and in the presence of an enzyme (Lu_c) is defined as 100% activity (Lu_t-Lu_c).The values of topo IIβ activity percentages versus a series of molecules concentrations are then plotted using non-linear regression analysis of sigmoidal dose-response curve. The IC_{50} value is determined using Graph pad Prism software. All experiments are repeated three times.

4.2.3. In vitro DNA immunofluorescence binding assay:

Histochemical immunofluorescence assay for establishing indirect DNA binding affinity is performed [29]. Briefly, slides of fixed MCF-7 cells are rinsed in three changes of PBS. Non-specific binding is prevented by incubation in blocking solution (10% fetal bovine serum in PBS) at 37◦C for 30 min. Slides are incubated for 30 min at 37◦C with pico-green dye solution (Abcam Inc., USA). Slides are rinsed again with PBS to remove excess dye, then treated with an ethanolic solution of the tested compounds **4b**, **9, 11**, **14** and PG at the concentration of their IC_{50} at 37 ◦C for 24 h. After washing, images are visualized at 642-645 nm by a fluorescence microscope (Axiostar Plus, Zeiss, Goettingen, Germany) installed with a camera (Power Shot A20, Canon, USA).

4.2.4. *In vitro* DNA- flow cytometry and Annexin staining analysis:

4.2.4a.DNA -flow cytometry analysis:

The MCF-7 cells are incubated at a density of 3 x10^6 cells/mL RPMI-1640 medium in T-75 flasks for 24 h and then treated with tested molecules **4b**, **9, 11**, **14** and PG at their IC_{50} (μM) for 24 h. The MCF-7 cells are then collected by trypsinization, washed with PBS and fixed. After that, treated cells are stained using the cycle test plus DNA reagent kit (BD Biosciences, San Jose, CA, USA) according to the manufacturer's instructions [30]. The percentage of cell cycle distribution is calculated using CELLQUEST software (Becton Dickinson Immuno-cytometry Systems, San Jose, CA, USA).

4.2.4b. Annexin staining apoptosis analysis.

The cells are cultured in a 10-cm plate for 24 h, after which IC_{50} concentration of tested molecules **4b**, **9, 11**, **14** and PG are added and incubated for up 24 h. Then, the cells are washed with PBS and detached by trypsin. The detached cells are collected into a 15-mL centrifuged tube, washed with ice-cold PBS twice, and centrifuge at 1200 rpm for 5 min. A volume of 0.1 mL binding buffer, is added to the treated MCF-7 cells, followed by adding 5 μL of annexin V-FITC and 5 μL of 50 μg/mL PI staining reagents. After mixing and reacting

at 25 °C for 15 min in the dark, the apoptotic cell percentages are analyzed by a flow cytometer. All experiments are done in triplicates.

4.2.5. *In vitro* EIISA immunoassay for p53 and cell death modulators:

The concentration of p53 protein and cell death modulators as Puma, Bax, Bcl-2 are measured using p53 ELISA kit, Puma ELISA Human (RAB0500), Human, Bcl-2 Elisa kit and Bax ELISA kit. The procedure is done according to the manufacturer's instructions. Briefly, lysates of MCF-7 cells are prepared from control and treated cells treated with IC_{50} concentration of the tested molecules. Then equal amounts of cell lysates are loaded then probed with specific antibodies. The optical densities are measured at 450 nm in ROBONEK P2000 ELISA reader. The experiments are done in triplicates.

4.2.6. *In vitro* green flow cytometry assay for active caspase 3/7 percentage:

The caspase 3/7 percentages are measured for the effect of tested molecules over MCF-7 cells in cell lysates using caspase-3/7 green flow cytometry assay kit (Cell Event), Catalog Number (C10427) per the manufacturer's instructions.

5-Acknowledgments:

The author is grateful to Dr. Al-Shorbagy MY. associate professor Pharmacology and Toxicology Department, Faculty of Pharmacy, Cairo University for statistical analysis of the data, Dr. Esam Rashwan, Vacsera, EGYPT, for performing p53 and cell death modulators assay, Dr. Enas. Ahmed Mohamed, associate professor of anatomy and embryology. Faculty of Medicine, Cairo University for measuring DNA histochemical immunofluorescence assay and BPS Bioscience Corporation (USA) for enzyme assay.

6- Conflict of Interest :

The author declares no conflict of interest.

7- Supplementary Materials :

The online version of this article contains supplementary materials.

8-References :

[1] Kumar, S., Ahmad, M.K., Waseem, M. & Pandey, A.K., *Med chem.,* 115-123(2015).

[2] Muthu K., Kathiravan Madhavi M., Khilare Aparna S.& Madhuri A., *J. Chem. Biol.* **6**, 25-36(2013).

[3] Hoelder S, Clarke P.A & Workman P., *Mol Oncol*., **6(2)**, 155-176(2012).

[4] Zhao L X., Kim T S., Ahn S H., Kim, T H., Kim E K., Cho W J., Choi H., Lee C S., Kim J A., Jeong TC., Change C. & Lee E.S., *Bioorg. Med. Chem. Lett.,* **11**, 2659-2662(2001).

[5] Hassanpour A., De Carufel C.A., Bourgault S. & Forgione P., *Chem. Eur. J.,* **20**, 2522-2528(2014).

[6] Ismail M., Arafa R K., Youssef M M. & El-Sayed W M., *Drug Des. Devel. Ther.,* 8, 1659-672(2014).

[7] Darshan N. & Manonmani H K., *J Food Sci Technol.,* **52(9)**, 5393-5407 (2015).

[8] Preya U H., Lee KT., Kim N J., Lee J Y., Jang D S. & Choi, J H., *Chem Biol Interact*. , **25(272),** 72-79 (2017)**.**

[9] Zhang H Z., Kasibhatla S., Kuemmerle J., Kemnitzer, Mason K O., Qiu L., Grundy C C., Tseng B., Drewe J. & Cai, S.X., *J. Med. Chem.***, 48(16),** 5215-23 (*2005*).

[10] Arthur Y., Shaw Meredith C. Henderson, Flynn G., Samulitis, B., Han H., Steve P. Stratton H.H., Chow S., Laurence H. Hurley & Robert T. D., *JPET*., **331**, 636-647(2009).

[11] Reines I., Kietzmann, M., Mischke R., Schering T., Lu A., Kleuser B. & Baumer, W., *J Invest Dermatol* ,**129**, 1954 -1962 (2009).

[12] Simoni D., Roberti M., Invidiata F.P., Rondanin R., Baruchello R., Malagutti C., ca Mazzali A., Rossi M., Grimaudo S., Capone F., Dusonchet L., Meli M., Raimondi M.V., Landino M., D'Alessandro N., Tolomeo M., Arindam D., Lu X, S. & Benbrook X., D.M., *J. Med. Chem.***, 44***,* 2308-2318 (2001).

[13] Kovačević S, Karadžić M, Podunavac-Kuzmanović S, Jevrić L, *Eur J Pharm Sci*.,1; **111,** 215-225 (2018).

[14] Boström J., Hogner, A., linàs A.L., Wellner E. & Plowright A.T., *J. Med. Chem.*, **55**, 1817-1830 (2012).

[15] Yang, L., *Breast Cancer and Molecular Medicine,* 841-858 (2006).

[16] Gu G, Dustin D & Fuqua SA., *Curr. Opin. Pharmacol.* , **31**, 97-103 (2016).

[17]. Suresh C. Ameta, Pinki B. Punjabi, Rakshit Ameta, Chetna Ameta. Microwave-assisted organic synthesis, *A Green chemical approach*, first edition, P 6-8 (2015).

[18] Mojtahedi M M., M. Saeed M.A., Mahmoodi P., & Adib M., *Synthetic Communications,* **1 (40)** ,2067-2074 (2010).
[19] Moeinpour F., Dorostkar N. & Vafaei M., *Synthetic Communications,***1(42)**, 2367-2374 (2012).
[20] Bai, R, Liu P, Yang J, Liu C & Gu Y., *ACS Sustainable Chem. Eng.*, ***3*** **(7)**,1292–1297 (2015).
[21] Abaee M. S., Hadizadeh A., Mojtahedi M.M., Halvagar M.R., *Tetrahedron Letters,* **58**, 1408-1412 (2017).
[22] Miles K.C., Mays S.M., Southerland B.K., Auvil T.J.& Ketcha, D.M., *ARKIVOC*, 181-190 (2009).
[23] Sylvain, R., Moult, Boulouard F, M., Max R., Béatrice G. & Michelle, D., *Eur. Pat. Appl*. EP0446133A1 (1991).
[24] Badran, M.M., Roshdy, S.M.A. & Mohammed K. Abd El-Hameid, *OCAIJ*. **9(11)**, 427-436 (2013).
[25] Outirite M., Lebrini M., Lagrenée M.& Bentiss F., *J. Heterocyclic Chem.,* **44**,1529-1531 (2007).
[26] Kaur N., *Synthetic Communications,* 3229-3247 (2014).
[27] Tolmachev A., Bogolubsky A.V., Pipko S.E., Grishchenko A.V., Ushakov D.V., Zhemera A.V., Iniychuk O.V., Konovets A.I., Zaporozhets O.A., Mykhailiuk P.K. & Moroz, Y.S., *ACS Comb. Sci.,* **18,** 616-624 (2016).
[28] Morgan DM., *Methods Mol. Biol*., **79**,179-83 (1998).
[29] Winston C. T. & Dale L. B., A, *Acc. Chem. Res*. **37**, 61-69 (2004).
[30] Zaki I, Abdel hameid M.K., El-Deen I M., Abdel Wahab A A., shmawy AM., Mohamed KO., *Eur. J. Med. Chem.***156**, 563-579 (2018).

Table 1: IC_{50} of carbonitriles **3a-c,** carboxamidamides **4a-c** and oxadiazoles **5-19** on MCF-7 cells (μM) and topo enzyme (nM).

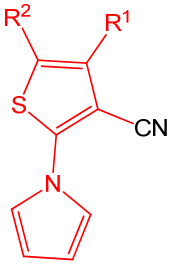

3a-c

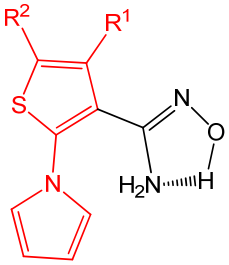

4a-c

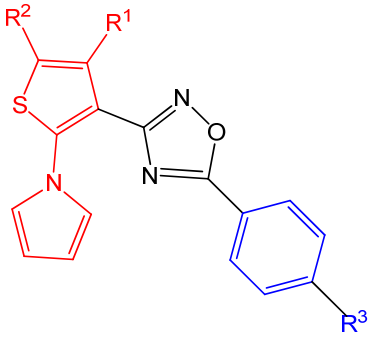

5-13

Code	R^1	R^2	R^3	MCF-7[a] IC_{50}(μM)[d]	HCT-116[b]	Topo[c] IC_{50} (nM)[e]
3a	$-CH_3$	$-CH_3$	-	19.45±1.61	NT	NT
3b	$-(CH_2)_4-$		--	16.10±1.10	NT	NT
3c	$4-CH_3OC_6H_4$	H	-	13.40±1.18	NT	NT
4a	$-CH_3$	$-CH_3$	-	5.98±0.41	NT	NT
4b	$-(CH_2)_4-$		-	4.52±0.43	10.52±1.03	123.49±9.41
4c	$4-CH_3OC_6H_4$	H	-	0.83±0.06	0.57±0.06	35.32±4.08
5	$-CH_3$	$-CH_3$	H	13.43±0.91	NT	NT
6	$-CH_3$	$-CH_3$	4-Cl	9.82±0.47	NT	NT
7	$-CH_3$	$-CH_3$	4-Br	8.64±0.81	NT	NT
8	$-CH_3$	$-CH_3$	$4-CH_3$	12.43±1.46	NT	NT
9	$-CH_3$	$-CH_3$	$4-OCH_3$	0.48±0.07	5.13±0.26	36.31±1.16
10	$-(CH_2)_4-$		H	12.94±0.92	NT	NT
11	$-(CH_2)_4-$		4-Cl	1.98±0.09	2.51±0.53	87.46±9.21
12	$-(CH_2)_4-$		4-Br	0.78±0.06	1.54±0.08	69.56±1.14
13	$CH_2)_4-$		$4-CH_3$	10.51±0.82	NT	NT
14	$-(CH_2)_4-$		$4-OCH_3$	0.19±0.05	1.17±0.09	27.28±1.11
15	$4-CH_3OC_6H_4$	H	H	13.76±1.10	NT	NT
16	$4-CH_3OC_6H_4$	H	4-Cl	12.11±1.11	NT	NT
17	$4-CH_3OC_6H_4$	H	$4-CH_3$	15.22±1.32	NT	NT
18	$4-CH_3OC_6H_4$	H	4-Br	15.62±1.31	NT	NT
19	$4-CH_3OC_6H_4$	H	$4-OCH_3$	21.80±1.71	NT	NT
PG	-	--	-	1.93±0.18	2.84±0.26	73.14±6.23

MCF7, [a] Human breast, HCT116, [b] Human colon cancer cell lines, Topo [c] , topoisomerase 2β enzyme, d, values are expressed as+ SEM (n: 3) in micromolar concentration and e , values mean + SEM (n=3) in nanomolar concentration . NT - Not tested.

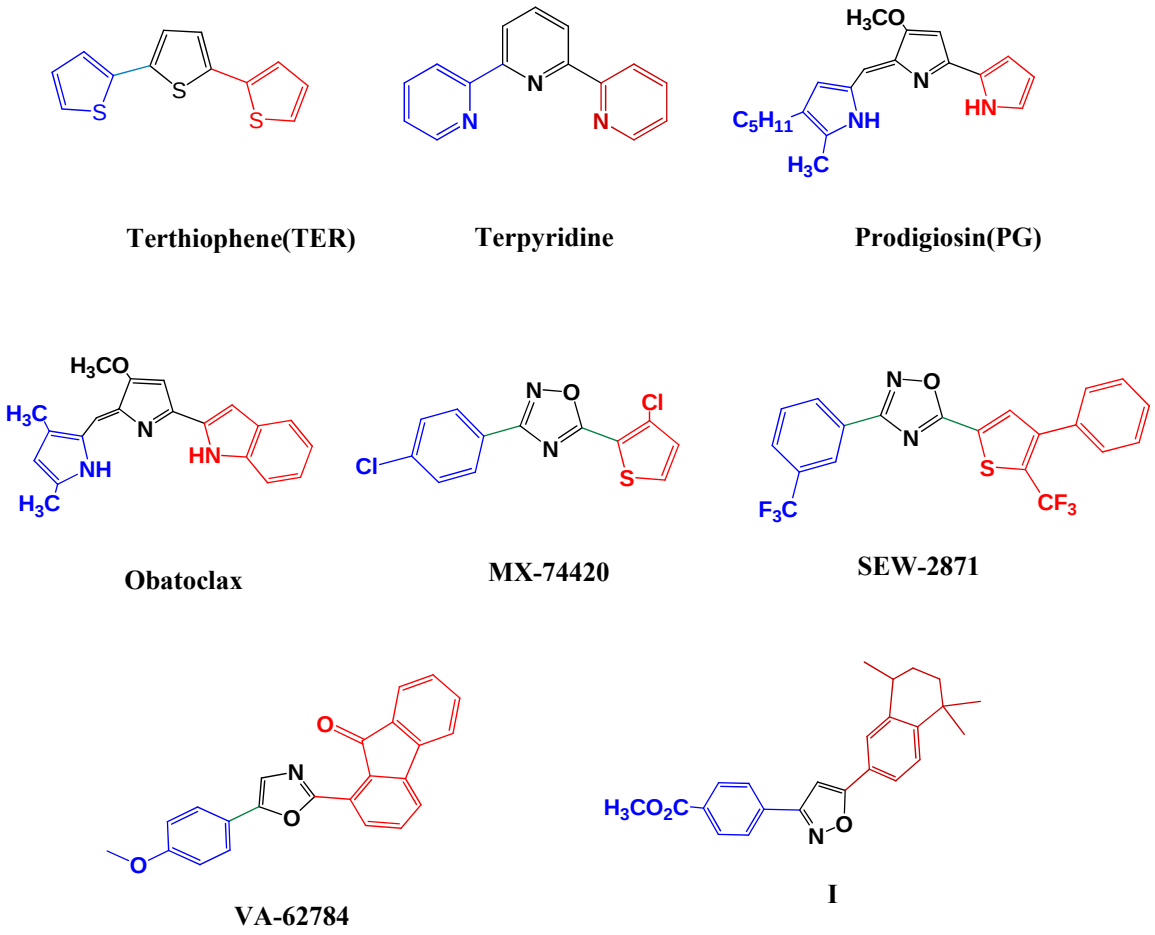

Fig. 1: Chemical structure of antitumor agents as orthogonal tricyclic molecules. Core rings is are shown in black color, bulky aryl groups are in red color and other small aryl groups are in blue color.
(Color figure can be accessed in the online version.)

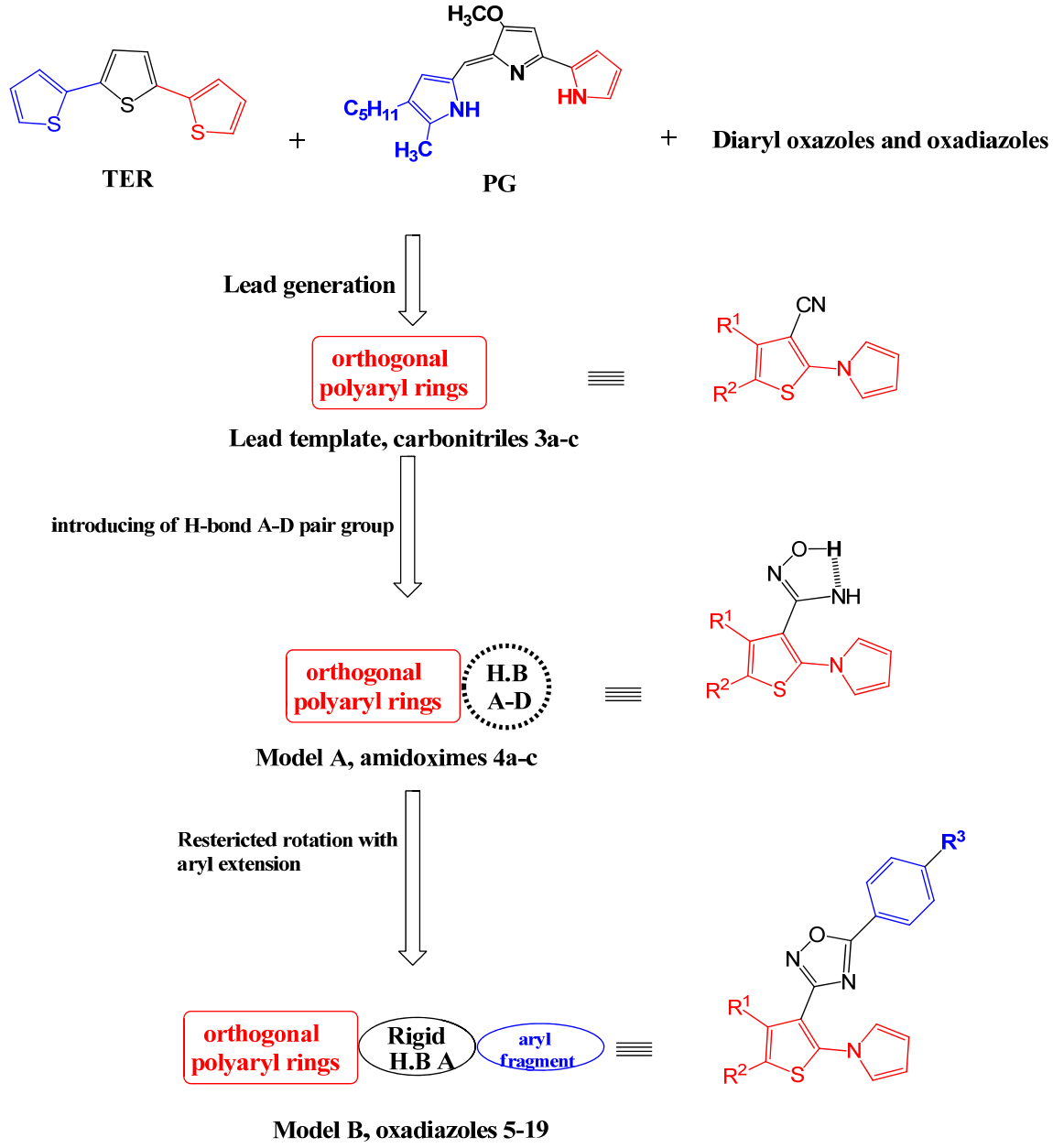

3a ,4a, 5-9, $R^1 = R^2 = CH_3$,
3b, 4b, 10-14, R^1, R^2 = $-(CH_2)_4-$,
3c, 3b, 15-19, $R^1 = 4\text{-}CH_3OC_6H_4-$, R^2=H, R

R^3= H, 4-Cl, 4-Br, 4-CH_3 , 4-OCH_3

H.B = hydrogen bond, A, acceptor, D, donor

Fig. 2: Diagrammatic sketch illustrate the design strategy. Orthogonal substituted polyaryl lead moieties are shown in red color, H-bond forming group and rigid oxadiazole core ring are in black color and small aryl fragments at C-5 of the core are in blue color.
(Color figure can be accessed in the online version.)

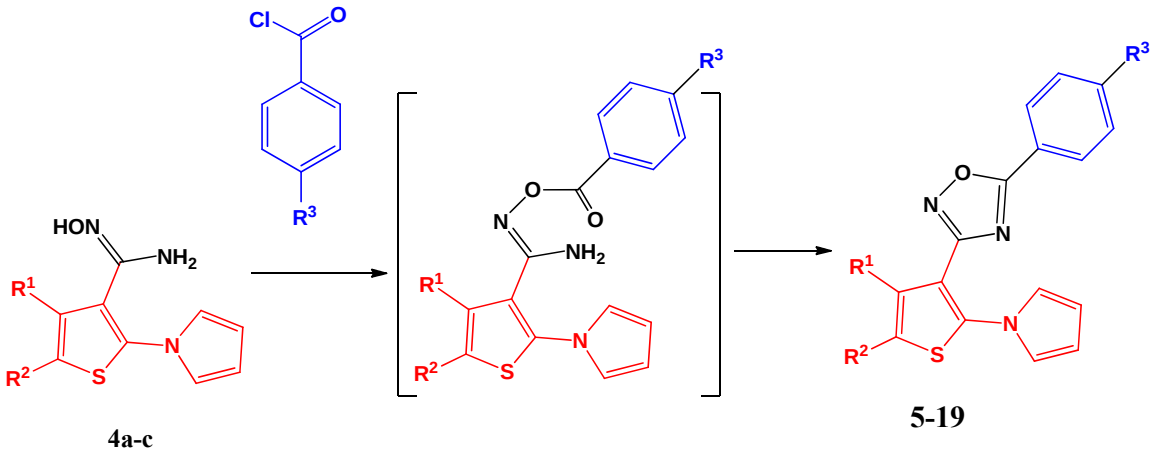

4a, R^1, R^2 = 2 CH_3, 4b, R^1, R^2 = - $(CH_2)_4$-, 4c R^1, R^2 =H, 4-CH_3O-C_6H_4

R^3 = H, Cl, Br, CH_3, OCH_3

Fig. 3: Sketch diagram represent the mechanism of formation of 3,5-diaryl oxadiazoles **5-19** from amidoximes **4a-c**.

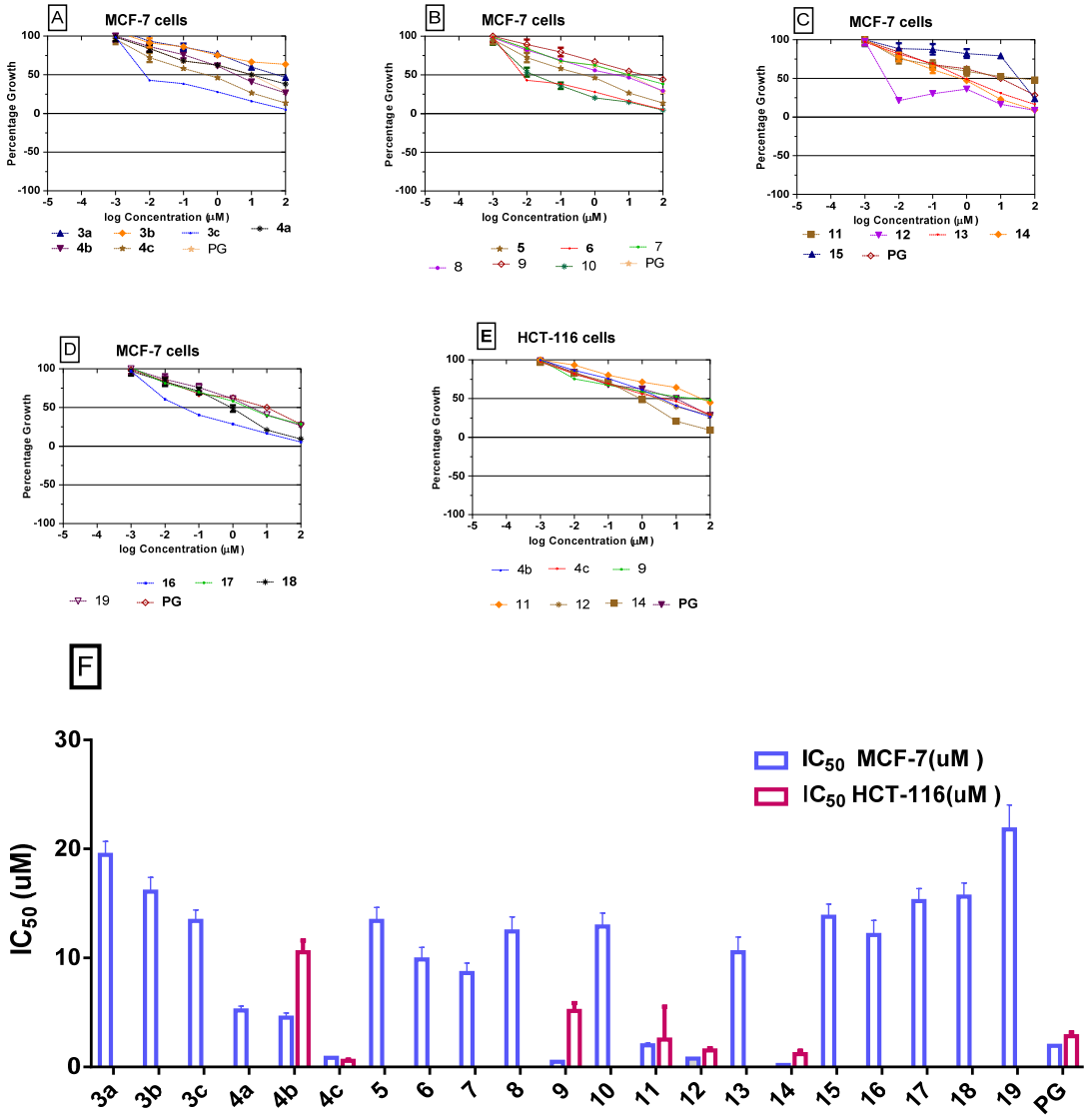

Fig. 4: Dose response curves for cell percentage viability of MCF-7cells, HCT-116 cells after treatment with tested molecules determined by MTT assay. A -D) Growth Inhibition effect of molecules on MCF-7 cells, E) Growth Inhibition effect of tested molecules on HCT-116 cells, F) Graphical presentation of the IC_{50} of tested molecules. Data is shown as mean + SEM (n: 3).

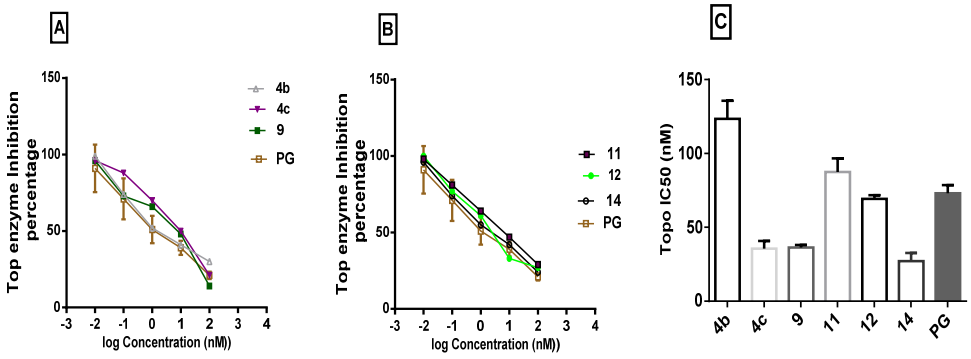

Fig. 5: A, B**)** *In vitro* 5 dose response curves for the determination of topo 2- β enzyme IC_{50} (nM) for molecules **4b**, **4c**, **9**, **11**, **12**, **14** compared with PG, C) Graphical presentation for comparison of IC_{50} for topo 2- β enzyme (nM) of the tested molecules and PG**.** The obtained data and are expressed as mean (n: 3) ± SEM.

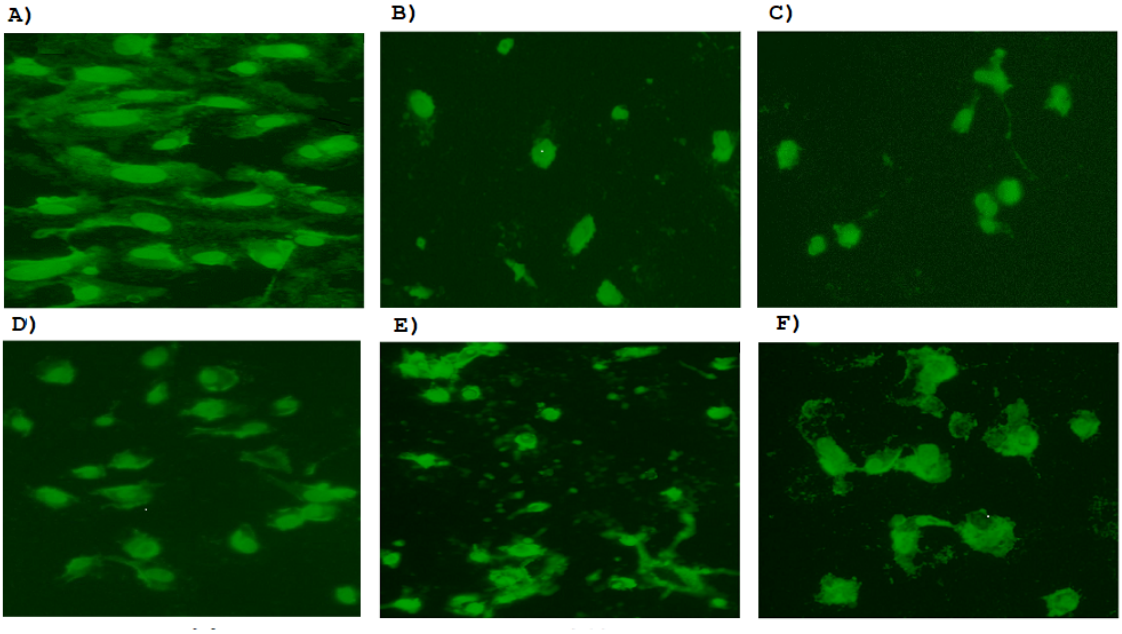

Fig. 6: Fluorescence intensity (IFU) of DNA indirect binding assay in MCF-7 cells for the effect of compounds **4b**, **4c**, **9** and **14** at their IC_{50} compared with PG as control for 24h**.** A) Untreated cells, B**)** Cells treated with of **4b** (4.52 µM), C**)** Cells treated with molecule **4c** (0.83 µM), D) Cells treated with molecule **9** (0.48 µM), E) Cells treated with molecule **14** (0.19 µM), F) Cells treated with PG (1.93 µM).

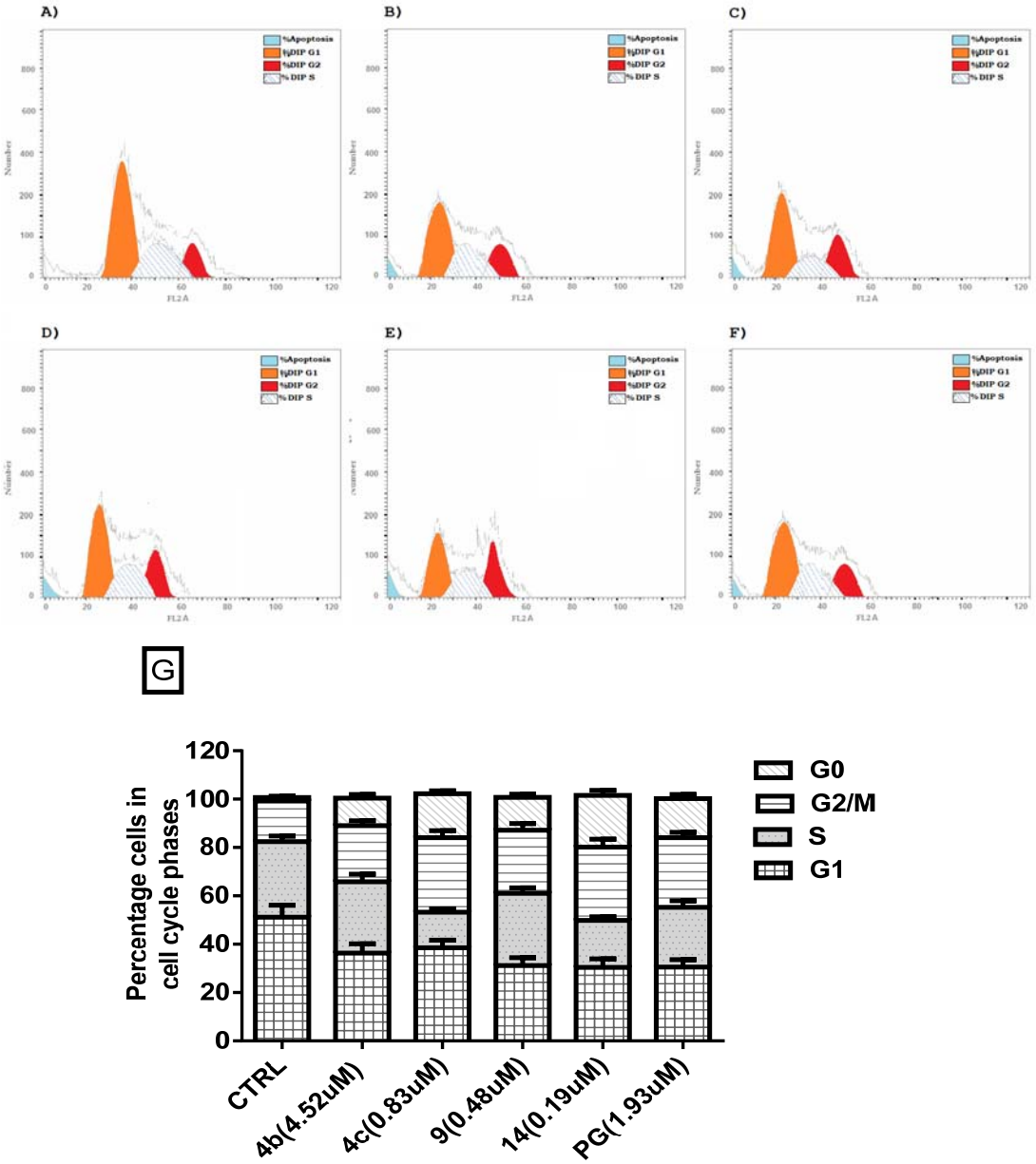

Fig. 7: DNA Flow cytometric analysis of the effect of molecule **4b**, **4c**, **9** and **14** at their IC_{50} on MCF-7 cells for 24h compared with PG, **A)** Control cells, B**)** Cells treated with of molecule **4b** (4.52 µM)**,** C**)** Cells treated with **4c** (0.83 µM), D) cells treated with **9** (0.48 µM), E) Cells treated with **14** (0.19 µM), F) Cells treated with PG (1.93 µM). G) Statically analysis of the obtained data and are expressed as mean (n: 3 experiments) ± SEM and statistical comparisons are carried out using one-way analysis of variance (ANOVA) followed by Tukey multiple comparisons.

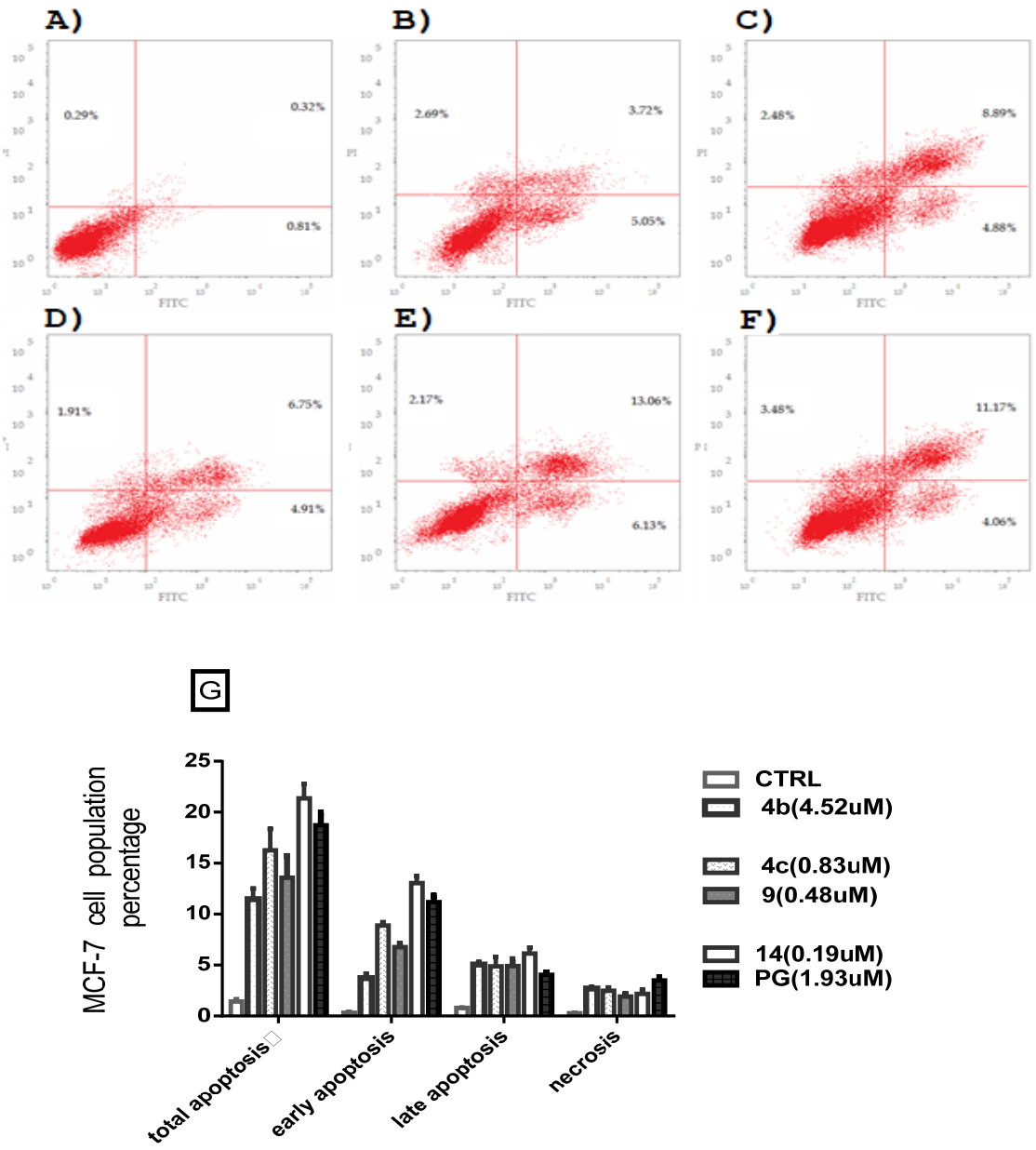

Fig. 8: Annexin V/PI analysis by flow cytometry of MCF-7 cells treated with molecules **4b**, **4c**, **9** and **14** at their IC_{50} compared with PG as e control for 24h. A**)** Control cells, B**)** Cells treated with of molecule **4b** (4.52 µM)**,** C**)** Cells treated with **4c** (0.83 µM), D) cells treated with **9** (0.48 µM), E) Cells treated with **14** (0.19 µM), F) Cells treated with PG (1.93 µM). G) Statistical analysis, data are expressed as mean (n: 3) ± SEM and statistical comparisons are carried out using one-way analysis of variance (ANOVA) followed by Tukey multiple comparisons. The red color represents the stained Annexin V cells.

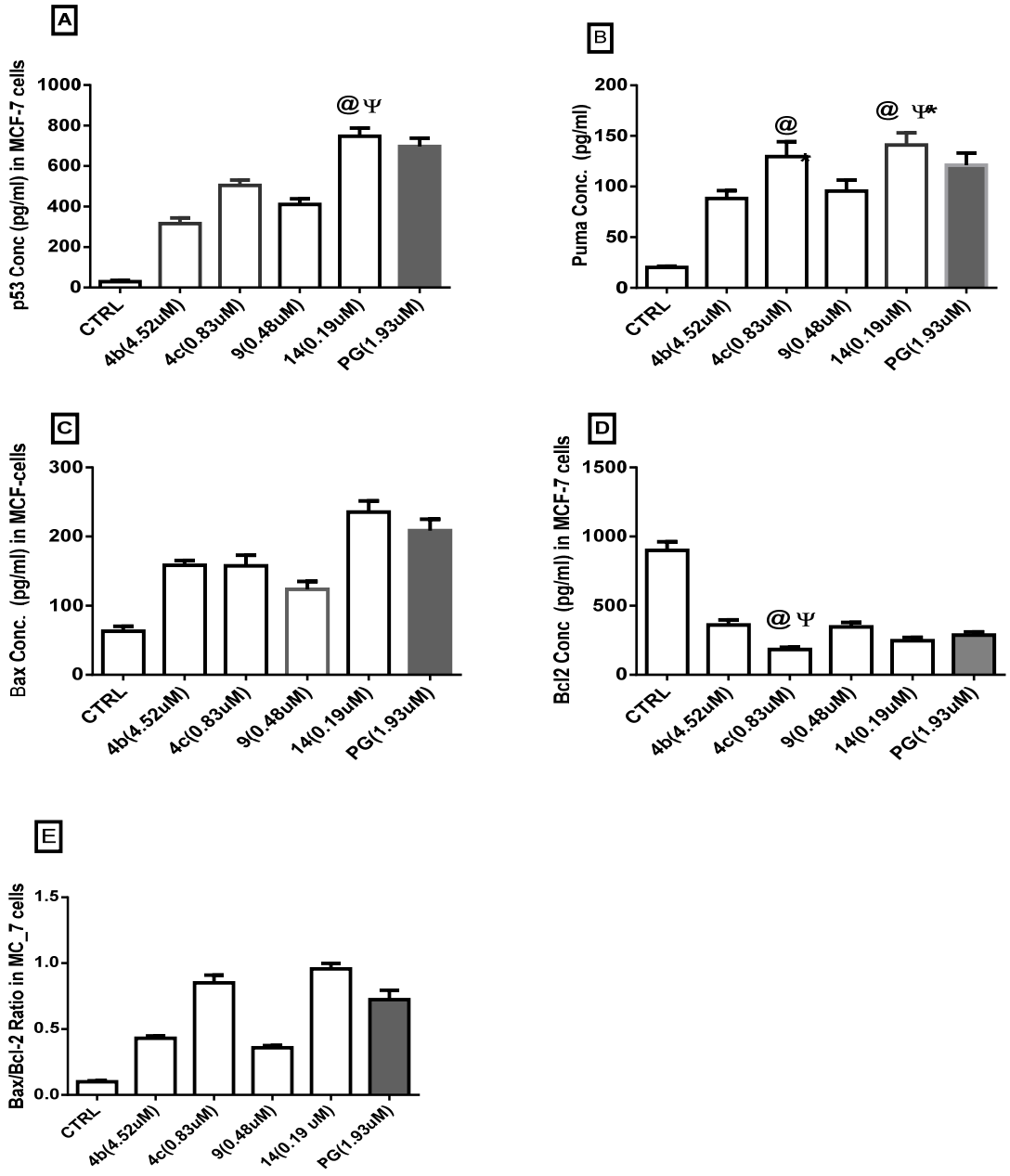

Fig. 9: ELISA-immunoassay for MCF-7 cells treated with molecules **4b, 4c, 9** and **14** at their IC_{50} compared with untreated cells and PG as positive control and untreated cells for 24h to measure the concentration of the following proteins, A**)** P53, B**)** Puma, C) Bax, D) Bcl-2, E) Bax/bcl-2 ratio. Data are expressed as mean (n: 3) ± SEM and statistical comparisons are carried out using one-way analysis of variance (ANOVA) followed by Tukey multiple comparisons at $p<0.05$ where Ψ as significant from CTRL, and @ as significant from PG .

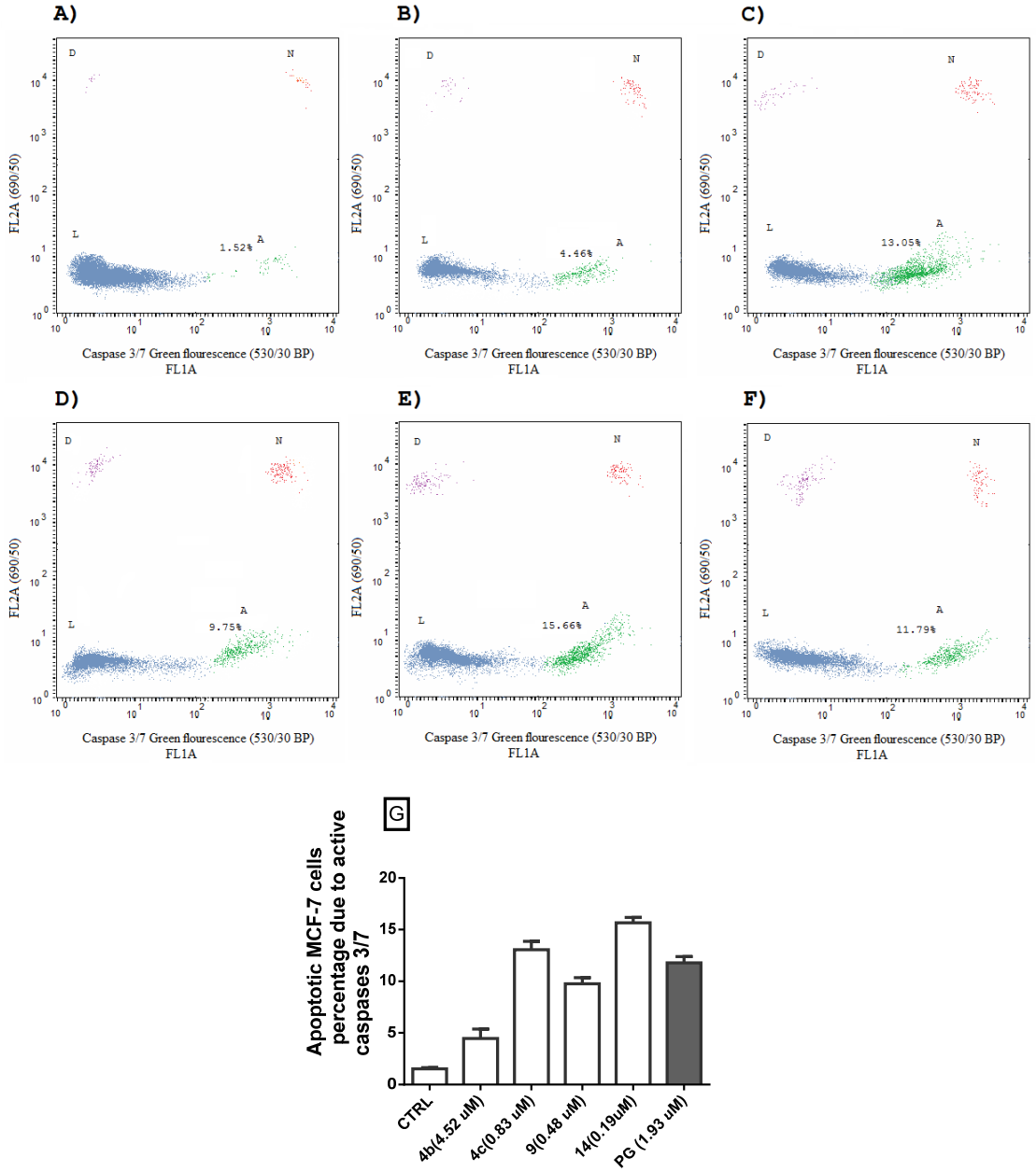

Fig. 10: Annexin V/pacific blue multicolor staining assay for MCF-7 cells after treatment with molecules **4b**, **4c**, **9**, **14** compared with PG for active caspase 3/7 and apoptosis induction after 24 h. A) Untreated cells, B) cells treated with **4b** (4.52 µM), C) Cells treated with 4c (0.83 µM), D) Cells treated with **9** (0.48µM), E) Cells treated with **14** (0.19 µM), F) Cells treated with PG (1.93uM). L: live cells (blue), A: apoptotic cells (green), N: necrotic cells (red), D: dead cells. **G)** Graphical presentation for comparison of apoptotic MCF-7 cells due to active caspases 3/7 percentages of the tested molecules and PG, Data represented as Mean ± SD of three independent trials**.**

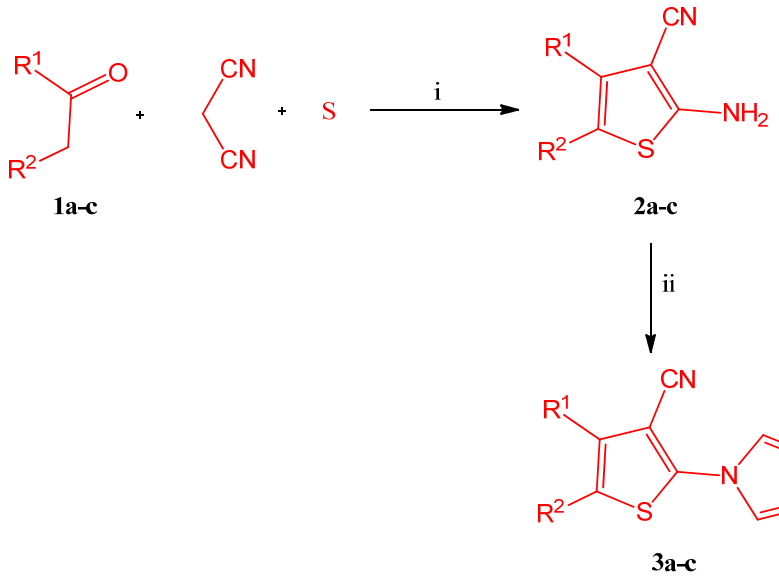

1a-c **2a-c** **3a-c**

2a) R^1, R^2= CH_3 **2b)** R^1, R^2=-$(CH_2)_4$- **2c)** R^1= 4-$CH_3OC_6H_4$, R^2= H

3a) R^1, R^2= CH_3, yield=74 % **3b)** R^1, R^2=-$(CH_2)_4$-, yield=81 % **3c)** R^1= 4-$CH_3OC_6H_4$, R^2= H, yield=76 %

Reagents & conditions: i) ***n*****-butanol, morpholine, 150^0 C , M.W, 10 min.**
ii) DMTHF, acetic acid, 100^0 C , M.W, 15 min.

Chart 1: Synthesis of 2-aminothiophenes **2a-c** and 2-(pyrrol-1-yl) thiophene-3-carbonitriles **3a-c.**

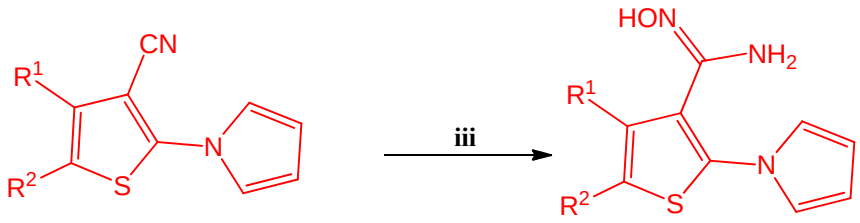

3a-c **4a-c**

4a) R^1, R^2= CH_3, **yield = 59%**

4b) R^1, R^2=-$(CH_2)_4$-, **yield = 67%**

4c) R^1=4-$CH_3OC_6H_4$, R^2= H, **yield = 58%**

Reagents & conditions: iii) $NH_2OH.HCl$, K_2CO_3, ***n*-butanol, 140 ^{0}C , M.W, 20 min.**

Chart 2: Synthesis of 2-(pyrrol-1-yl) thiophene-3-carboximidamides **4a-c.**

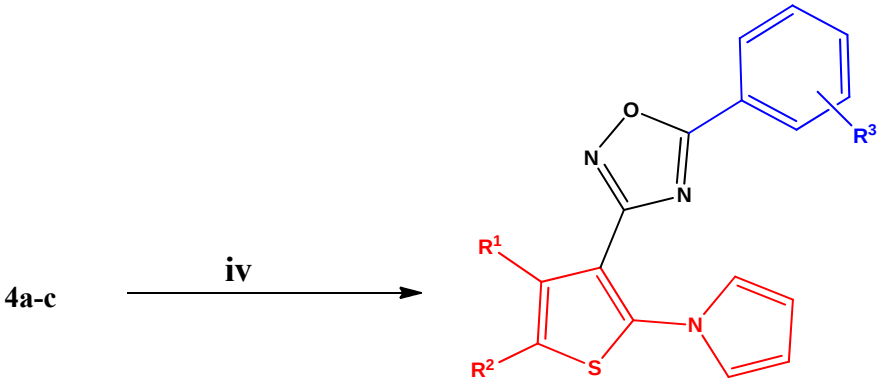

5-19

5) R^1=R^2= CH_3, R^3=H, yield=75 %

6) R^1=R^2= CH_3, R^3=4-Cl, yield=55 %

7) R^1=R^2= CH_3, R^3=4-Br, yield=59 %

8) R^1=R^2= CH_3, R^3=*4*-CH_3, yield=49 %

9) R^1=R^2= CH_3, R^3=4-OCH_3, yield=56 %

10) R^1&R^2=-$(CH_2)_4$-, R^3=H, yield=79 %

11) R^1&R^2=-$(CH_2)_4$-, R^3=*4*-Cl, yield=63 %

12) R^1&R^2=-$(CH_2)_4$-, R^3=4-Br, yield=66 %

13) R^1&R^2=-$(CH_2)_4$-, R^3=4-CH_3, yield=60 %

14) R^1&R^2=-$(CH_2)_4$-, R^3=4-OCH_3, yield=58 %

15) R^1= 4-$CH_3OC_6H_4$, R^2= H, R^3=H, yield=71 %

16) R^1= 4-$CH_3OC_6H_4$, R^2= H, R^3=4-Cl, yield=59 %

17) R^1= 4-$CH_3OC_6H_4$, R^2= H, R^3=*4*-Br, yield=65 %

18) R^1= 4-$CH_3OC_6H_4$, R^2= H, R^3=4-CH_3, yield=58 %

19) R^1= 4-$CH_3OC_6H_4$, R^2= H, R^3= 4-OCH_3, yield=46 %

Reagents & conditions :iv , acid chloride, ethylene glycol, 200 C^0 , M.W, 5 min.

Chart 3: Synthesis of 5-aryl-3-(2-(1H-pyrrol-1-yl)-thiophen-3-yl) 1, 2, 4-oxadiazoles **5-19.**